A review of structural responses and design of offshore tubular structures subjected to ship impacts

Zhaolong Yu [a, b*], Jørgen Amdahl [a, b]

a, Department of Marine Technology, Norwegian University of Science and Technology (NTNU), Norway

b, Centre for Autonomous Marine Operations and Systems (AMOS), Norwegian University of Science and Technology (NTNU), Norway

Abstract

Over the past decades, the offshore oil and gas industry has developed rapidly. A large number of offshore structures, notably jacket and jack-up platforms, were constructed and installed worldwide. As they are often exposed to safety threats from impacts by visiting vessels and dropped objects, there has been a continuous interest in understanding the impact mechanics of tubular structures and proposing practical design standards to protect from collisions. This paper reviews the state-of-the-art with respect to the response dynamics and mechanics of offshore tubular structures subjected to mass impacts, covering material modelling, ship impact loading, energy absorption in the ship and platform, global and local responses of tubular structures, the residual strengths of damaged tubular members and design considerations to mitigate against ship impacts. A wealth of information is available in the literature, and recent findings and classical references, which have a wide influence, are prioritized. The collected information is compared and discussed. The findings in this paper will help understand the impact response of offshore tubular structures and assessment procedures, and provide useful indications for future research.

Key words: ship collisions; offshore tubular structures; impact mechanics; local and global responses; residual strength; design considerations

* Corresponding author, Dr. Zhaolong Yu; Email: zhaolong.yu@ntnu.no

Contents

Nomenclature

L	Length of the tubular member
D	Diameter of the tubular member
D_{min}	Refer to Fig. 14(c) and (d)
D_{max}	Refer to Fig. 14(c) and (d)
t	Tube wall thickness / Time
B	Contact width of the indenter
ξ	Transverse extension of damage along the tube length
w	Lateral deflection of the leading generator
w_b	Beam deflection of a tubular member
w_d	Indentation depth
$w_{d,tran}$	The transition indentation from local denting to global bending
σ_{dyn}	The dynamic stress
σ_{stat}	The quasi-static stress
σ_y	Yield stress of the tube steel material
σ_u	Ultimate stress of the tube steel material
σ_{dp}	Initial plastification stress of a damaged tube under compression
E	Young's modulus / Dissipated energy
F_{max}	The maximum collision force for a ship structure crushing into a rigid tube
K	A constant coefficient representing the shape of the indenter in Eq. (5)
k_s	Tangential stiffness of the force-deformation curve of the ship
k_i	Tangential stiffness of the force-deformation curve of the installation
$m_0=1/4\sigma_y t^2$	Plastic bending moment of tube wall per unit width
M_p	Plastic bending capacity of the tube cross section
M_{res}	Residual bending capacity of a dented cross section
N	The axial loads (positive in compression)
N_p	Plastic yield resistance in tension
N_{sd}	Design axial compressive load
N_{rd}	Design axial compressive resistance
R	Lateral deformation resistance of tubular members
R_c	Characteristic denting resistance factor
R_0	Plastic bending collapse load of a tubular member with fixed ends
$R_{0,eff}$	Effective bending collapse load of a dented tubular member with fixed ends
R_s	Deformation resistance of the ship in Eq. (29)
R_i	Deformation resistance of the installation in Eq. (29)
R_d	The design resistance of the structure
S_d	The design load acting on the structure
γ_1	Effective bending capacity coefficient of tube cross sections at the ends
γ_2	Effective bending capacity coefficient of a dented tubular cross section
λ_R	Column slenderness parameter
C	The Cowper-Symonds constant (s^{-1})
p	The Cowper-Symonds constant

1. Introduction

Ships and offshore structures operating at sea are exposed to risks of ship collisions and impacts from dropped objects. Potential consequences may vary from minor local structural deformation to major threats to structural integrity, causing great economic loss, severe environmental pollutions and fatalities. In extreme conditions, accidental loads may cause the global collapse of entire structures and put human lives in jeopardy. The huge losses from several catastrophic marine collision accidents such as the sinking of the *Titanic* after hitting an iceberg and explosion of the Mumbai High North platform after suffering a collision from a supply vessel, have aroused continuous public concern regarding the operational safety of ships and offshore structures. Tremendous efforts have been made mainly in two directions:

1) to reduce the probability of occurrence of ship collisions with the application of advanced navigational tools and administration procedures.
2) to obtain crashworthy design of structures based on a thorough understanding of fundamental collision mechanics.

Based on research outcomes, rules and standards relevant for the design of crashworthy structures have been introduced, e.g., DNV-RP-C204 (2010), ISO 19902 (ISO, 2007), API-RP2A-WSD (2014), ABS (2013) and HSE (2004). The standards have been continuously updated to include novel knowledge and address new challenges.

A few review articles are available in the literature, and they mainly focus on general procedures of risk analysis and structural assessments in ship collisions and groundings (Ellinas and Valsgard, 1985; Moan and Amdahl, 1989; Pedersen, 2010; Wang et al., 2002). However, no specific review exists that addresses the complicated collision mechanics of tubular structures. The authors consider it highly important that reseachers understand the theories and principles developed over the long time span, so that they can provide a solid foundation for future research works. It is therefore the purpose of this paper to bridge the gap in knowledge by presenting a comprehensive review of structural response assessments and design considerations specifically for offshore tubular structures in the accidental limit states (ALS), covering both classical references and more recent progress as well. The review focuses especially on the NORSOK N-004 code and the DNV-GL recommended practices for design against accidental loads because they contain the most detailed provisions.

Design against extreme ship collision should be carried out in the accidental collapse limit state using risk based techniques (Moan, 2009). The probability of system loss due to a collision of a certain intensity (kinetic energy) at a given location may be calculated as the product of the probability of collision with a given intensity and location multiplied with the probability of damage for the given event and the probability of system loss conditioned on the calculated damage of the structure subjected to relevant permanent loads and environmental loads. It is necessary to integrate over all possible collision intensities and locations. The calculated probability of system loss shall comply with the target safety level. The target safety level considering all kinds of accidents implies a probability level for system loss in the range of 10^{-4} per year for ALS according to NORSOK N003 (NORSOK, 2017). With approximately ten different accidental categories, collision accidents should therefore have an annual failure

probability of 10^{-5}. Taking that into account, the characteristic values are used for loads and resistance. The conditional probability of failure for structures nominally at the brink of collapse is estimated to be in the range of 0.1 (Moan, 2009).

In practice, it is very cumbersome to calculate the probability of failure for all intensity levels and locations. Simplifications are necessary. It has therefore become customary to design the structure by a deterministic analysis of ship collisions with an annual probability of occurrence of 10^{-4}. Thus, characteristic kinetic energy is typically determined via risk analysis as adopted in ship-ship collisions analysis (Pedersen, 2010).

The design collision event that has been used for decades is the impact from a standard supply vessel with a displacement of 5000 tons travelling with a speed of 2 m/s based on risk analysis. This gives a design energy of 11 MJ for bow impacts and 14 MJ for broad side impacts considering added mass effects (DNV-RP-C204, 2010). Over the years, kinetic energy has increased significantly with the increased ship displacements and impact velocities identified in Moan et al. (2017) and Kvitrud (2011) based on an overview of collision accidents in recent years. Moreover, newly designed ship structures such as bulbous bows, X-bows and ice strengthened vessels may change impact consequences. According to the new version NORSOK N003 standard (NORSOK, 2017), if no operational restrictions on allowable visiting vessel size are implemented, supply ship displacements should not be selected less than 10, 000 tons, and unless further evaluations are performed, the kinetic energy should be 50 MJ for bow impacts, 22 MJ for stern impacts and 28 MJ for broad side collisions. This represents a substantial increase in the demand for collision resistance of an offshore structure.

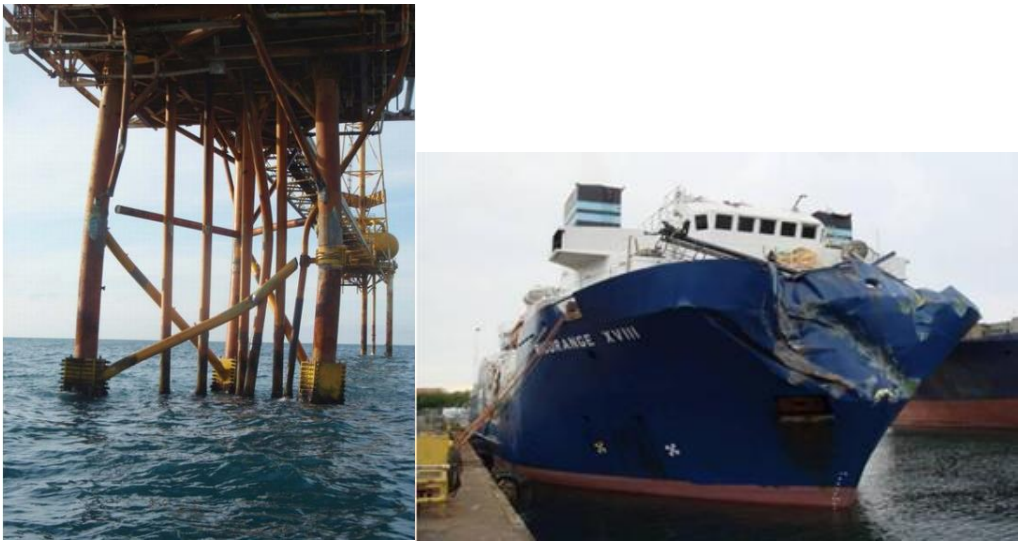

Fig. 1. Big Orange-Ekofisk 2-4/W collision (source: PSA (2009))

The design scenarios of the new version NORSOK N003 standard with increased design energy may be classified as high energy collisions. Under high impact energies, tubular members will undergo significant deformations and may fracture and fail, threatening the integrity of the platform. A noticeable example is the well workover vessel Big Orange XVIII collision with the Ekofisk 2/4 jacket platform, in which the estimated kinetic energy was 60 MJ. The accident

caused severe damage to the three-legged jackets and also to the bow (see Fig. 1). Several braces were ruptured, and the jacket had to be dismantled. Such high collision energies cannot be absorbed by a single member. It is therefore essential to design tubular members such that they have sufficient strength to penetrate the bow, and the ship bow absorbs considerable energy (Amdahl and Johansen, 2001).

Minor ship collisions and dropped objects often occur and cause small damage to the platform braces and legs. According to Taby (1986), operational damages occurring almost every year for North sea jackets are a dent depth of 10% of the tube diameter and/or a permanent deflection of $0.004L$, where L is the span length of the member. As timely repair of a damaged offshore structure is difficult and expensive, it is important to have knowledge about the ultimate and post-ultimate strength of damaged tubular members under various loading conditions so as to make optimal decisions regarding safety and economy. A good illustration of minor ship collisions and subsequent damage assessment, safety evaluation, and repair was reported by Sveen (1990) when a West German submarine collided with the eight-legged Oseberg B jacket on the Norwegian Continental Shelf in 1988 with an estimated energy of 5-6 MJ (refer to Fig. 2). The struck diagonal brace absorbed 60 percent of the energy and suffered major damage with a large local dent and overall deflection. A safety assessment of the undamaged and damaged platform was carried out using nonlinear finite element analysis (NLFEA). The simulated accelerations and strain responses compared reasonably with data measured using the platform monitoring system during the collision. The collapse analysis of the damaged platform revealed high reserve strength in jacket structures. Repairs to the platform by replacing the damaged brace were also reported.

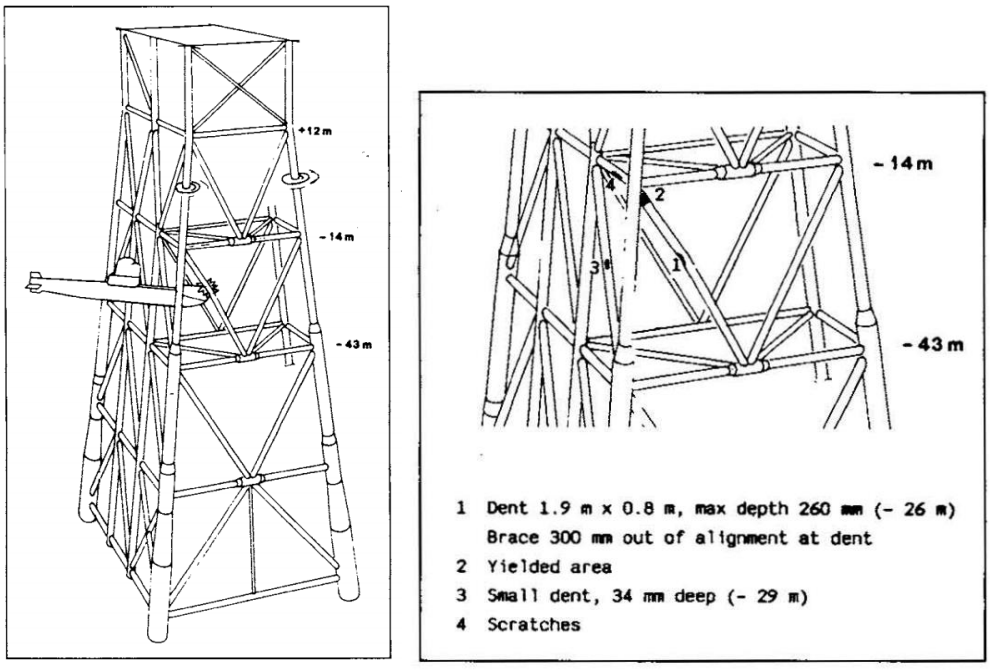

Fig. 2. The collision scenario and damage to structures; from Sveen (1990)

The responses of offshore tubular structures subjected to ship impacts are complicated from various aspects, e.g., local and global structural responses, the residual strengths of damaged members and structures, the behavior of tubular joints, and static and dynamic effects. From the perspective of energy dissipation, the total energy should be dissipated through damage to both the ship and the platform. There can be significant ship-platform interactions depending on the relative strengths of both structures. Another important consideration for collisions is the response of braces and legs. Braces or legs in direct contact with a ship will undergo three deformation stages, which are local denting, global bending and membrane stretching (see Fig. 3), and different deformation stages may interact. Depending on tube dimensions, material properties and boundary conditions, tubular members behave quite differently, and deformations are governed by different patterns. For example, local denting dominates for short tubular members with large diameter over thickness ratios (D/t), and global bending dominates for long tubes with small D/t ratios. However, most tubes are likely to sustain damage due to combined local denting and overall bending. Braces and legs in the vicinity of a struck member will also deform and absorb energy. Supporting braces subjected to axial compression may buckle and dissipate energy during collisions, especially when a ship strikes platform joints. In view of the considerable number of aspects of the problem and their complexities, ship collisions with offshore tubular structures remain a topic under intensive research and may become increasingly important as vessels grow larger.

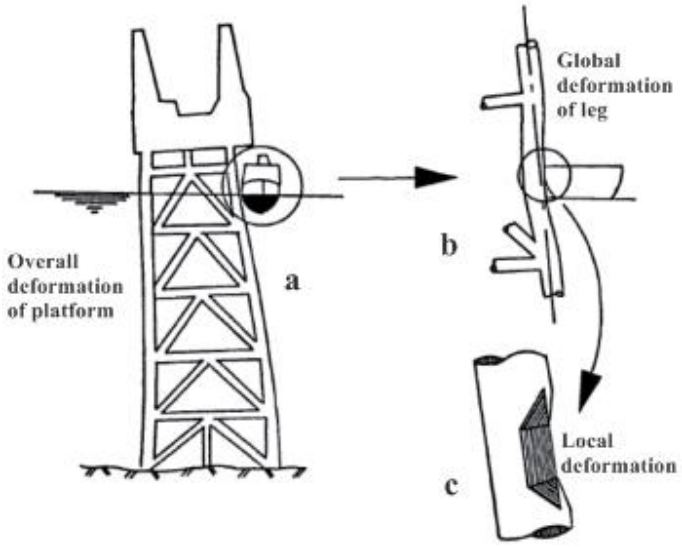

Fig. 3. Energy absorption of steel jackets, from Amdahl (1980)

The aim of this work is to review the state-of-the-art impact response mechanics of offshore tubular structures and the design of crashworthy tubular structures. The review includes nine principal sections. *Section 2* introduces the methods for ship collision assessments and discusses material modelling and fracture. *Section 3* presents typical ship impact loadings on offshore tubular structures. *Section 4* reviews the global impact responses of offshore tubular structures. In *Sections 5 and 6*, the responses of single tubular members subjected to lateral impacts (*Section 5*) and axial compression (*Section 6*) are extensively discussed. *Sections 7* and 8 deal with the responses of tubular joints and ultimate strengths of damaged tubes, respectively. *Section 9*

addresses the design of crashworthy offshore tubular structures. *Section 10* concludes the review and indicates potential topics of interest for future research.

2. Methods for ship collision assessments

2.1 Analysis methods

The analysis and design of offshore structures subjected to ship impacts requires reliable and efficient analysis tools for predicting structural damage and residual strength of damaged structures. Full scale experiments or model tests are considered to be the most straightforward and accurate method if the scaling law is properly handled. NLFEA methods have shown powerful capabilities to assess structural responses in ship collisions using coarsely meshed shell elements. The commonly used general-purpose NLFEA packages include LS-DYNA (Hallquist, 2006), ABAQUS (Hibbitt et al., 2001) and MSC/DYTRAN, ANSYS. USFOS (Soreide et al., 1999), which is a special-purpose software based on beam-column analysis, is also available for efficiently and accurately predicting damage and collapse of offshore structures. USFOS follows the idea of the Idealized Structural Unit Method (ISUM) proposed by Ueda and Rashed (1984) and Ueda et al. (1985). In the method, a structure is divided into the largest "structural units" possible and the geometric and material nonlinear behaviors are described in a concise analytical-numerical form. Simplified analytical methods based on plastic analysis are often preferable in the design stage as they provide quick and reasonable predictions of structural resistance and damage and provide significant details on the underlying mechanics of structural responses. In addition, the resulting equations often have a simple form and are well suited to be written into design standards regarding accidental actions.

In order to select a proper method for ship collision analysis and design, it is essential for analysts and designers to balance the required accuracy, computational time and modelling efforts while considering the pros and cons of each method as follows:

- Experimental methods are useful for impact analyses of one or a few tubular members, but impact experiments with entire platforms can hardly be undertaken. Real impacts, such as the Big Orange-Ekofisk 2-4/W collision, yield valuable information though.
- Simplified methods are by their very nature simple and are useful for the preliminary design and rapid assessment of structural responses, but the global response of a platform is difficult to capture.
- NLFEAs employing beam-column models (e.g. USFOS) are capable of predicting the global response of a platform with substantially reduced computational time and resources compared to shell analysis and still with reasonably good accuracy. The detailed local damage is, however, not provided, and ship-platform interactions with increasing contact area are not captured. An improvement to this may be to find an empirical correction factor, which is a function of dent depth and tube diameter.
- NLFEAs employing shell elements and explicit solutions methods (e.g., LS-DYNA and ABAQUS) are capable of predicting both local and global responses of struck platforms and capturing ship-platform interaction effects, but the required modelling effort for platforms and ships are subtantial, and computational time will be large. Significant

efforts may be needed to calibrate models against code capacities for e.g. joints/local buckling, etc, especially for residual strength assessments in damaged conditions.

2.2 Modelling material behavior and fracture

Steel offshore constructions are generally designed to perform an optimum bewteen the two poles of safety and reliability on one hand, and economy on the other hand. Fixed offshore structures are conventionally constructed from medium grade structural steels with yield strengths that are typically 355 MPa. Meanwhile, high strength steels with yield strengths of 420-500 MPa are being increasingly applied due to their good performance with respect to increased strength to weight ratio and attendant savings in material costs and construction schedules (Billingham et al., 2003). The steel grades are well documented in rules and standards such as DNV-OS-B101 (2009), NORSOK-M-120 (2008), BS-EN-10225 (2009), ABS-MODU (2012), etc. Even higher strength steels (>550 MPa and often up to 700 MPa) are also applied in mobile jack-up drilling rigs (Billingham et al., 2003). As the demand for lightweight offshore structures with high energy absorption capacities increases significantly, an increasing tendency to use high strength steels can be expected. Particular concerns regarding the application of high strength steels are, however, their greater susceptibility to hydrogen cracking, fatigue and fracture.

The mechanical behaviors of isotropic steel materials can be described by the complete stress-strain curves from tensile tests, as plotted in Fig. 4. The engineering stress-strain curve includes the linear elastic stage, plastic yielding, a yield plateau, strain hardening, necking, postnecking softening and fracture. This should be converted to a true stress-strain curve with proper corrections on postnecking softening in order to be used in NLFEA. The strengths of steel are likely to be influenced by the strain rates and ambient temperature as well. Construction steels possess substantial ductility due to strain hardening and are capable of absorbing considerable energy after the initial yielding. The performance of steel ductility may be evaluated with the yield ratio σ_y / σ_u, which is defined as the initial yield stress over the ultimate stress, and the elongation at fracture. Mild steels, which have low yield ratios and large elongation percentages at fracture, generally have better ductility performance than high strength steels, referring to Fig. 4, whereas Billingham et al. (2003) stated that modern clean steels with low carbon contents and low levels of impurities may experience significant elongations even at high strength and high yield ratios. In simplified analytical analyses, steel materials are often assumed to be rigid perfectly plastic, neglecting strain hardening for simplicity, and this is conservative. If materials with no hardening or little hardening are used in real construction, the structures are, however, likely to develop localized deformations (e.g., local hinges) and trigger early fracture.

The strain rate effect in ship collisions is complicated. On one hand it increases the initial yield stress and plastic flow stress of the material, which is beneficial. On the other hand, the increased stress level is believed to reduce steel ductility and trigger a possible transition from ductile to brittle fracture. However, recent experiments (Choung et al., 2013; Li and Chandra, 1999) have shown that the elongation at fracture could either increase with higher strain rates or not have an obvious dependence. This was, however, for tension coupon specimens that did not include cracks/weld defects.

A widely used model for ship collision analyses was developed by Cowper and Symonds (1957), in which the strain rate effect was accounted for by scaling the static stress with a dynamic hardening factor (DHF):

$$\sigma_{dyn} = \sigma_{stat}\left[1+\left(\frac{\dot{\varepsilon}}{C}\right)^{\frac{1}{p}}\right] \tag{1}$$

where $\dot{\varepsilon}$ is the strain rate, and C and p are parameters that are calibrated from experiments. Cowper and Symonds (1957) suggested $C = 40.4\,s^{-1}$ and $p = 5$ for the initial yield stress of mild steels based on experiments. Paik and Thayamballi (2003) recommended $C = 3200\,s^{-1}$ and $p = 5$ for the initial yield of high strength steels. Jones (1989) stated that the C parameter should be linearly dependent on plastic strains, whereas Choung et al. (2013) suggested to relate it to the plastic strain squared. Storheim and Amdahl (2017) showed that calibrations based on initial yield stress would overestimate collision resistance significantly and suggested calibrating the model to the plastic flow stress. Nevertheless, ship collisions normally occur at relatively low speeds (smaller than 10 m/s), and the effect of strain rate on the structural response is generally limited. In view of the considerable uncertainties related to strain rate effects and how to include them in a realistic manner, it is recommended that the effect be disregarded in analyses of ship collisions with offshore structures. Another important issue is the low temperature conditions for ships and offshore structures working in arctic regions. Kim et al. (2016) carried out material tensile tests and dropped object tests at room temprature and a low temperature of -60 °C and found that the strength of steels became stronger at low temperatures and that brittle fracture may occur.

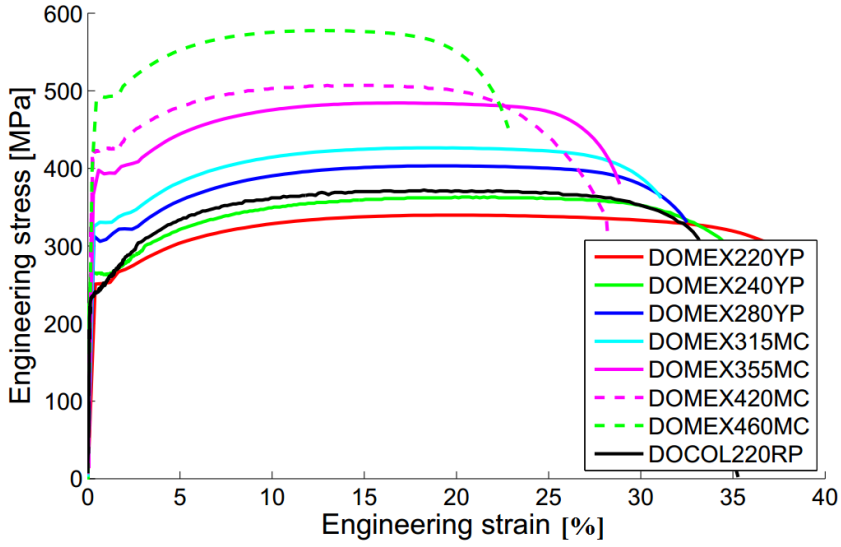

Fig. 4. Uniaxial tensile test data from the database of SSAB, from Storheim (2016)

To conduct realistic and reliable ship collision simulations with NLFEA, it is essential to correctly calibrate material behavior into idealized material models. The isotropic power law

hardening model with a yield plateau is often used to describe steel behavior. A range of input parameters need to be determined, most of which have significant statistical variability and the evaluations require a high degree of craftsmanship. VanDerHorn and Wang (2011) conducted a significant statistical study on the material properties of shipbuilding steels gained from approximately 140,000 tensile tests. The data were collected from five manufacturers delivering steels for ABS-class ships during 2004-2009. The importance of considering the statistical uncertainties of steel material properties were indicated. The probabilistic density distributions of the yield and ultimate stresses and percent elongations of different steel grades were presented. Hogström and Ringsberg (2012) studied the influence of uncertainties of the input material parameters on the shape and size of damage to a struck ship, and showed that the scattering of material properties and the choice of fracture criterion would lead to large differences in the outcome of the analysis.

A recent benchmark study (Ringsberg et al., 2018) was initiated by the MARSTRUCT virtual institute for modelling buckling and fracture of structures with NLFEA, where 15 groups of well-establihed researchers worldwide were invited to simulate the indentation response of a side shell structure and simulation results were compared to experiments. The results showed significant scattering with respect to collision resistance and energy absorption owing to the adopted different strategies for structure modelling, material calibration, numerical settings and fracture criteria, etc. Recent efforts by DNV-GL with the new version DNV-RP-C208 (2016) are dedicated to mitigating such uncertainties in assessments of nonlinear structural responses. Guidance or requirements are provided for many of the challenging aspects. Storheim et al. (2017) stated that when evaluating the material strength of a body, it is good practice to assess whether a high or low strength is more unfavorable for the object in question. In ship collisions, for example, the most unfavorable combination is a high material strength of the striking vessel and a low material strength of the struck vessel. Typically, the characteristic resistance of a body should represent a 5% probability that the resistance is less than the specified value. The revised DNV-RP-C208 (2016) opts for the characteristic resistance with a lower fractile for the struck vessel and mean values for the striking vessel, which seems like a reasonable approach to obtain a combined 5% fractile (Storheim et al., 2017).

Another big challenge is to accurately capture material fracture initiation and propagation with coarsely meshed shell elements. The complexity lies in that fracture is a localized phenomenon on the length scale of plate thickness and is difficult to capture with large shell elements, the sizes of which are several times larger than the plate thickness. In addition, fracture depends highly on stress states, material deformation history and is sensitive to the mesh size adopted. It is essential to correctly calibrate the material properties in order to accurately capture strain localizations and subsequent fracture. The probabilistic nature of material properties makes fracture modelling even more complicated. Quite a few fracture criteria exist in the literature for structures modelled with large scale shell elements. The BWH (Bressan-Williams-Hill) criterion (Alsos et al., 2008) and the RTCL (Rice–Tracey and Cockcroft–Latham) fracture criterion (Tørnqvist, 2003) may be recommended as they generally show reasonable and consistent predictions in several benchmark studies (Calle et al., 2017; Ehlers et al., 2008; Marinatos and Samuelides, 2015; Storheim et al., 2015) with various small and large scale tests. Refined fracture models are needed for further studies.

3. Ship impact loading

Offshore structures may potentially suffer collisions from ships of different types including visiting vessels such as supply vessels, and passing vessels, e.g., oil tankers, containerships, bulk carriers, submarines and passenger ships. The different ship types with different displacements and structural designs yield quite different ship impact loadings on the struck structures. For offshore structures struck by visiting attendant vessels, the current DNV-RP-C204 (2010) recommends a design supply vessel with a displacement of 5000 tons, and the corresponding design force-deformation curves for broad side, bow and stern impacts are shown in Fig. 5. Many of the curves were based on simplified analytical methods when they were derived. The recently updated version of the DNV RP C204 standard (DNV-GL, 2018) (to be released) has accounted for new features of increased ship displacements, new ship bow designs and ice strengthed structures. The recommended force-deformation curves for standard design vessels with displacements of 6,500-10,000 tons are shown in Fig. 6. The design resistance increases significantly compared to the old version curves. For supply vessels with bulbous bows, the force-deformation relationship for bow impacts of the design vessels is given in Fig. 7 with both no ice reinforcements and ICE-1C class. Force-deformation curves for bow impacts of a design oil tanker (125,000 dwt) and a design Very Large Crude Carrier VLCC (340,000 dwt) are also recommended in the updated version of the DNV RP C204 standard (DNV-GL, 2018).

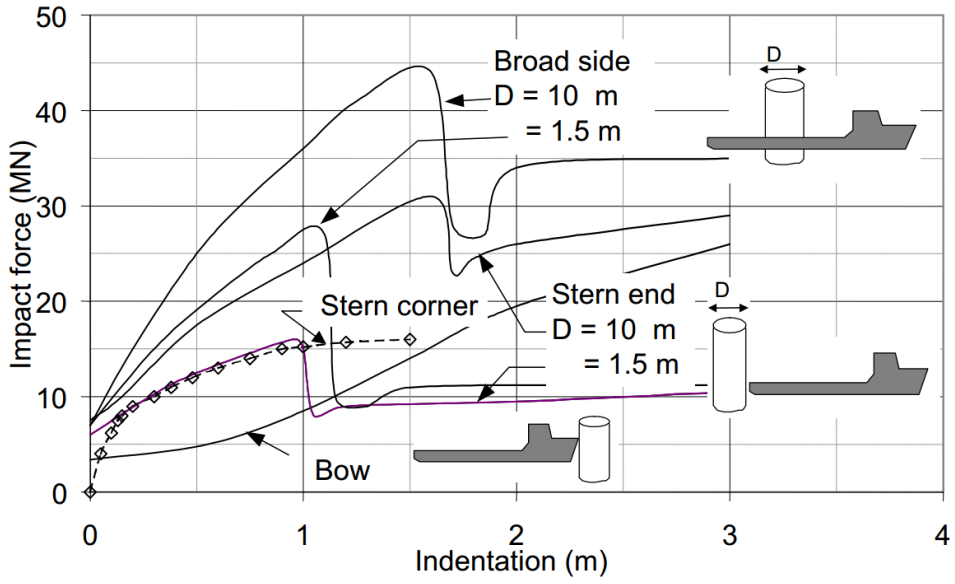

Fig. 5. Recommended force-deformation curves for the standard vessel with a displacement of 5000 tons in beam, bow and stern impacts (DNV-RP-C204, 2010)

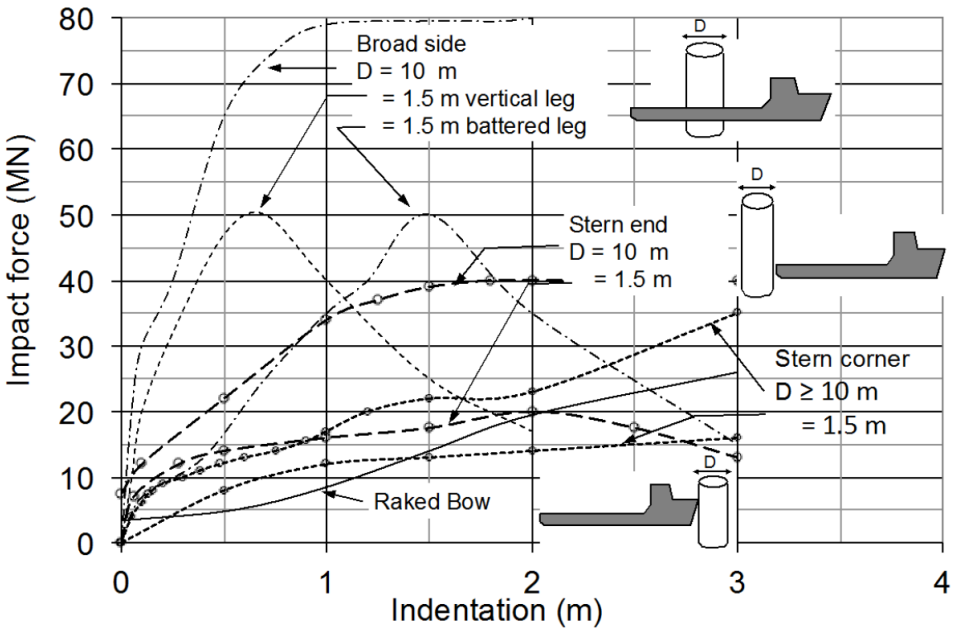

Fig. 6. Recommended force-deformation curves for standard design vessels with displacements of 6500-10,000 tons in beam, bow and stern impacts; (DNV-GL RP C204 standard, version 2018)

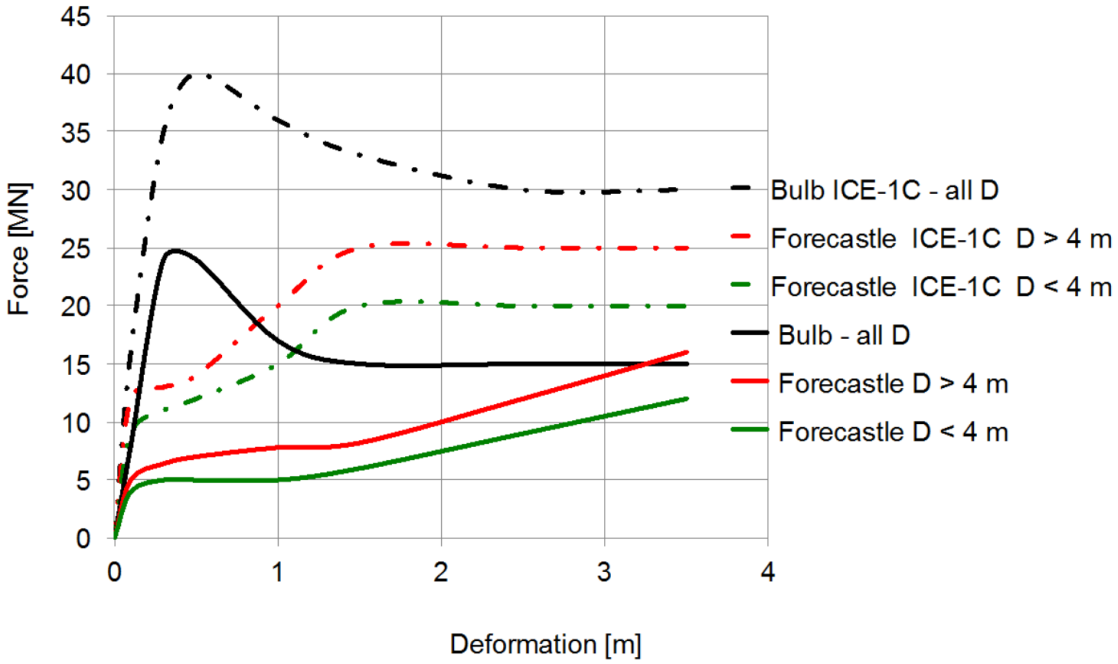

Fig. 7. Force-deformation relationships for bow impacts from supply vessels with displacements of 5,000-10,000 tons, standard bulbous bows with no ice reinforcement and with ICE-1C class. (DNV-GL RP C204 standard, version 2018 (DNV-GL, 2018))

The curves presuppose that the impacted structure does not undergo substantial deformation, such that the strength design requirements are complied with. If this condition is not met, interactions between the bow and the impacted structure shall be taken into consideration, referring to Haris and Amdahl (2013).

For a specific ship given structural details and material properties, NLFEA may be carried out to accurately predict the ship indentation resistance. Alternatively, simplified methods can be used to obtain a rapid assessment of ship crushing resistance with reasonable accuracy. This normally applies to ship collisions with ship sides, FPSOs or large-diameter columns. Minorsky (1958) presented pioneering work that empirically related the energy absorbed in ship damage to the volume of damaged material based on full-scale ship collision data. The regression fit the data quite well in the high-energy impact regions for conventional ships, but the model can be questioned when applied to modern designed ships. Simplified analytical models for the crushing of plated structures, notably ship bows, can generally be categorized into two groups, i.e., the intersection unit method and the plate unit method, according to Yamada and Pedersen (2008). The intersection unit method follows the suggestion by Gerard (1958) to divide complicated plated structures into basic intersecting units such as L-, T-, and X elements (see Figs. 8 (a, left) and (b)). Examples of the intersection unit method are Amdahl (1983), Yang and Caldwell (1988), Ohtsubo and Suzuki (1994), etc. The plate unit method was proposed by Paik and Pedersen (1995), where the structures are divided into separate plate units; refer to Figs. 8 (a, right) and (c). More details can be found in the benchmark study carried out by Yamada and Pedersen (2008), in which simplified methods for the axial crushing of plated structures were reviewed, and predicted crushing resistances by different models were compared with a series of large-scale tests on the axial crushing of bulbous bow models. In addition, shell plates may be subjected to stretching and develop significant membrane forces. Simplified models for laterally struck shell plates are found in Jones et al. (1970) and Zhu (1990), and more recently in Haris and Amdahl (2012) and Sun et al. (2015) for ship sides.

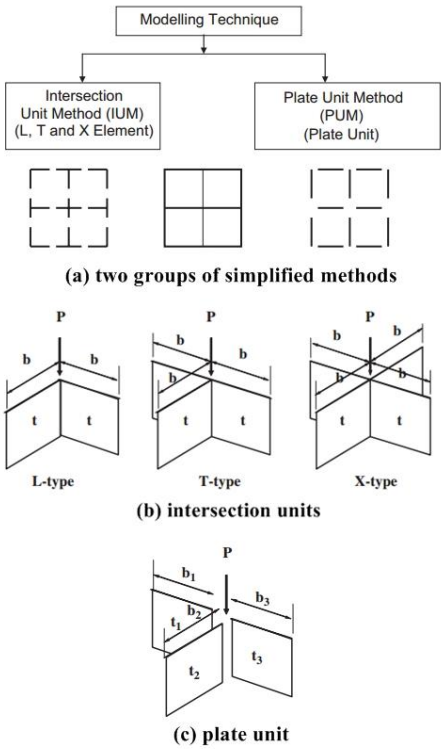

Fig. 8. Simplified methods for the axial crushing of plated structures; from Yamada and Pedersen (2008)

4. Global response of offshore platforms

4.1 Energy dissipation

During a collision, part of the kinetic energy will be absorbed through plastic straining, structural motion and vibrations, and hydrodynamic dissipation by accelerating added masses. Depending on the collision angle and relative position, some kinetic energy may remain after the collision. Often, ship collision assessments are carried out in two steps, i.e. analyses of external dynamics and internal mechanics, as first suggested by Minorsky (1958). *External dynamics* deals with global motions of the striking and struck bodies before, during and after collisions and predicts total energy absorption in the structures. This energy should be dissipated in the *internal mechanics* analysis through structural deformations of the two colliding bodies.

Regarding energy dissipation in ship-ship collisions, the elastic energy of ship hull girder vibrations is often considered to be negligible. This was proved to be reasonable by Pedersen and Li (2009), and they showed that elastic energy absorbed by *the struck ship* through global hull girder vibrations was normally small and varied from 1% to 6% of the energy released in crushing. Based on the conservation of momentum, Pedersen and Zhang (1998) proposed a closed form solution for energy dissipation in ship collisions considering planar surge, sway and yaw motions. Stronge (2004) developed a solution for impacts of rigid bodies considering 6DOF motions. Liu and Amdahl (2010) reformulated Stronge's 6DOF model in a local coordinate system for ship collisions, which allowed objects with three dimensional geometries and eccentricities such as icebergs to be considered. The accuracy of the external dynamics models was discussed by Tabri (2012) and Yu et al. (Yu and Amdahl, 2016; Yu et al., 2016a; Yu et al., 2016b) by comparison with coupled simulations. The external dynamic models were found to be capable of predicting energy dissipation at the end of the first impact with good accuracy in general. The prediction accuracy tended to decrease for cases with small collision angles and long durations. Possible secondary impacts caused by periodic motions were not captured. The input normal vector of the tangential contact plane for the 6DOF external dynamic model should be determined with care. If the struck object is able to cover the striking ship bow, ship motions may potentially be locked by structural deformations. The use of the normal vectors of the undamaged structural surfaces may not give the correct predictions.

The coupled simulation model developed by Yu et al. (Yu and Amdahl, 2016; Yu et al., 2016a; Yu et al., 2016b) is capable of capturing hydrodynamic forces, 6DOF ship motions and structural damage simultaneously but virtually does not increase computational time (the time for calculating hydrodynamic forces is negligible compared to that for structural response calculations). Fig. 9 shows results from a coupled simulation of a supply vessel colliding with a vertical jacket leg (20 × 2 × 60, length [m] × diameter [m] × thickness [mm]), with an impact kinetic energy of approximately 60 MJ. The trajectories of several representative nodes were recorded. The ship rolled anticlockwise initially with large collision forces and bending moments and rolled back after some time under the action of the water restoring forces. The complex 6DOF ship motions and structural deformations were well captured. It was observed that the external dynamic models by Pedersen and Zhang (1998) and Liu and Amdahl (2010) may fail to work for ship collisions with braces and legs, because a leg would penetrate deep into the striking vessel structure and the striking ship motions would then be locked to some extent by the local

deformations. In such cases, the assumption of rigid body collisions sharing a common tangential plane at the contact surface of the colliding bodies is no longer valid, and the dissipated energy is much underestimated. A similar phenomenon can be expected when a strong ship bow penetrates a weak ship side at an oblique collision angle. More information on the discussion of accuracy of external dynamic models can be found in Yu (2017) and Yu and Amdahl (2017).

For offshore jackets and jack-up platforms in relatively deep water, the first natural periods may become comparable to typical ship impact durations, and the elastic energy absorbed by platform motions needs to be accounted for. This is especially the case for jack-up platforms, which are characterized by large natural periods and limited stiffness against lateral deflections. Pedersen (2013) and Zhang et al. (2015) proposed a simplified model for assessing the external dynamics of ship collisions considering global motions of the struck object like wind turbines, quays, bridges, and jack-up rigs; see Fig. 10. Platform motions in the transverse direction were considered. The platform was found to absorb much less plastic energy compared to that assuming pure rigidity. The model may be further developed to consider rotational motions in eccentric collisions.

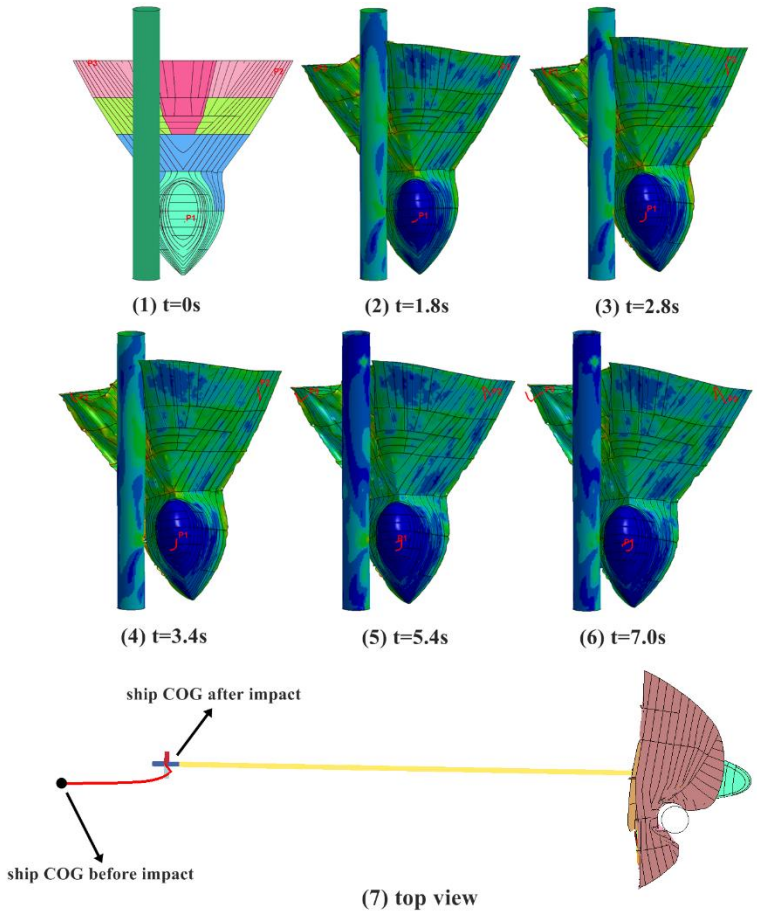

Fig. 9. Coupled simulation of a supply vessel colliding with a jacket leg

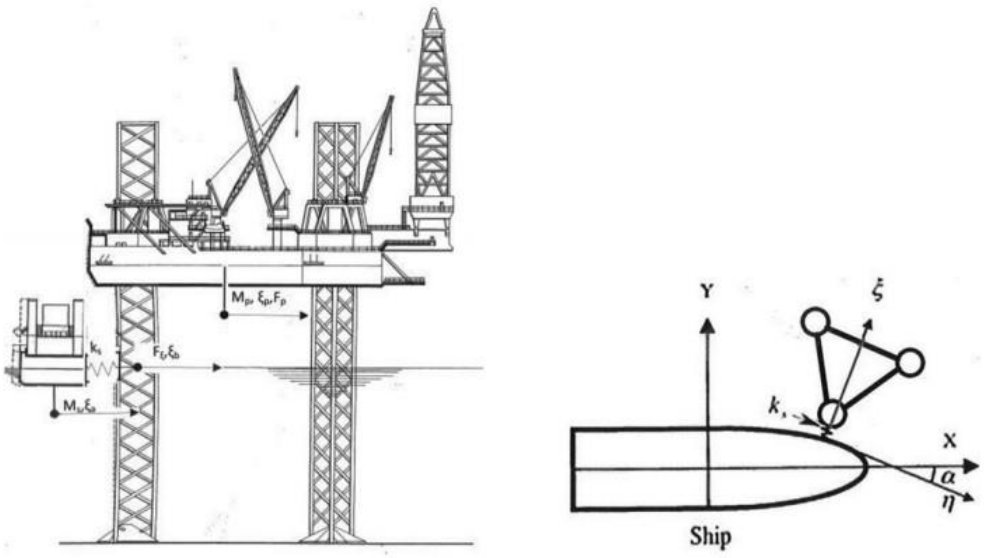

Fig. 10. A simplified model for a supply vessel impacting a chord of a jack-up platform from Zhang et al. (2015).

NLFEAs are often carried out when the global response of platform becomes important. Petersen and Pedersen (1981) studied a ship swaying into a fixed jacket platform using a code that they developed. They found that the global elastic energy of the platform was considerable when the platform had either a very large or a very small dynamic stiffness compared to the collision forces. Travanca and Hao (2015) simulated quite a few ship collision cases with three different jacket platforms using LS-DYNA. The platforms were modelled with shell elements. They found that global elastic deflection energy could be important for jackets, especially for large platforms. The portions of global elastic energy out of total energy were large for ship collision with strong legs and tubular joints, which have large local stiffness at the impact point. Travanca and Hao (2014a) simulated ship collisions with jacket and jack-up platforms using LS-DYNA with shell elements and simplified the platform global response with equivalent single-degree-of-freedom (SDOF) systems. They found that the equivalent SDOF models were able to simulate global deflections of the platforms generally well. However, in eccentric collisions, both the lateral and torsional responses were prominent for the jack-up platforms. Equivalent models in such cases should account for both lateral and torsional responses. The rotational reponses were found to be less important for jackets in the studied cases. In a different study by Travanca and Hao (2015), rotational stiffness was found important for a tripod in eccentric collisions. Amdahl and Holmas (2016) analyzed the response of a typical jack-up subjected to a high-energy collision of 67 MJ on a corner leg using USFOS (Soreide et al., 1999). The platform was installed at a water depth of 110 m, and the first eigenperiod was 7.8 s. It was found that the ship spent considerable time in the elastic unloading phase (1.9 - 5.2 s), and up to 25 MJ was stored as elastic energy mainly in the platform during impact. The inertia force was important, and the temporal impact force depended on the jack-up response, which could not be calculated a priori. The compliance of the platform contributed significantly to the survival of the impact and needed to be considered.

4.2 Static and dynamic responses in ship-platform collisions

Collisions between offshore platforms and boats are complex problems. Many approaches exist with varied simplifications for predicting the impact responses of vessels and platforms. Gjerde et al. (1999) compared methods to assess the response of jack-ups to boat impact and provided recommendations regarding their levels of accuracy. Simplified equations were found to be reasonable when structural failure was governed by failure of the impacted member or connected adjacent members that were incorporated in hand calculations. For cases where structural failure was not governed by failure of the impacted member, the energy absorption capabilities of the platform were underestimated by the simplified methods. More accurate predictions were obtained through static and dynamic NLFEAs of the entire platform.

The dynamic effects in ship-platform collisions may be classified into two parts: the local effect and the global effect. The local dynamic effect is characterized by the strain rate sensitivity of the material and the inertia effect of the impacted and adjacent members. The influence of the local dynamic effect is found to be generally limited in the normal range of ship impact velocities. Based on drop hammer test results (Jones et al., 1992) on clamped-end tubular members with varied impact velocities up to 14 m/s, Jones and Shen (1992) concluded that the quasi-static approach yielded errors generally smaller than 10 percent when the striking mass was at least approximately four times larger than the beam mass, provided a different failure mechanism was not activated. More recently, Zhang et al. (2018) conducted similar tests and found that dynamic hardening amplification was generally below 10 percent up to 10 m/s. A further increase in impact velocity to 13 m/s, however, yielded a much larger dynamic hardening increase of around 20 percent.

The global dynamic effect activates the global motions of the platform structure, which is especially important for jack-ups. During collisions, the platform deck must be accelerated and there is a large force going up to the deck. There is a response lag of the deck compared to the hit region due to the large inertia of the deck, and the force may be calculated assuming support at the deck. In a static approach, the force is smaller because of deck displacement. Fig. 11 shows the dynamic response of a jack-up platform subjected to ship side collisions at the time instants of the maximum collision force and the maximum displacement. The analysis was carried out by Amdahl and Eberg (1993) using USFOS. The displacements were magnified by a factor of 20. It was easily observed that the platform deck was virtually unmoved when the maximum collision force was reached. In the USFOS dynamic analysis, the resistance to penetration of the ship bow was modelled with a nonlinear spring. Fig. 12(a) shows a force-end shortening curve for the spring that was reproduced in the simulation as input, and the resulting collision force history is shown in Fig. 12(b). It is observed that the ship spent considerable time in the elastic unloading phase and that the platform received a significant impulse during this phase. The impulse depended significantly on the unloading stiffness adopted, which should be realistically estimated. Amdahl and Eberg (1993) also found that three factors could be crucial to the dynamic effects: the local strength of the platform relative to the ship, the duration of the collision relative to the fundamental period of the governing motion, and the strength of the members transmitting forces needed to accelerate the deck.

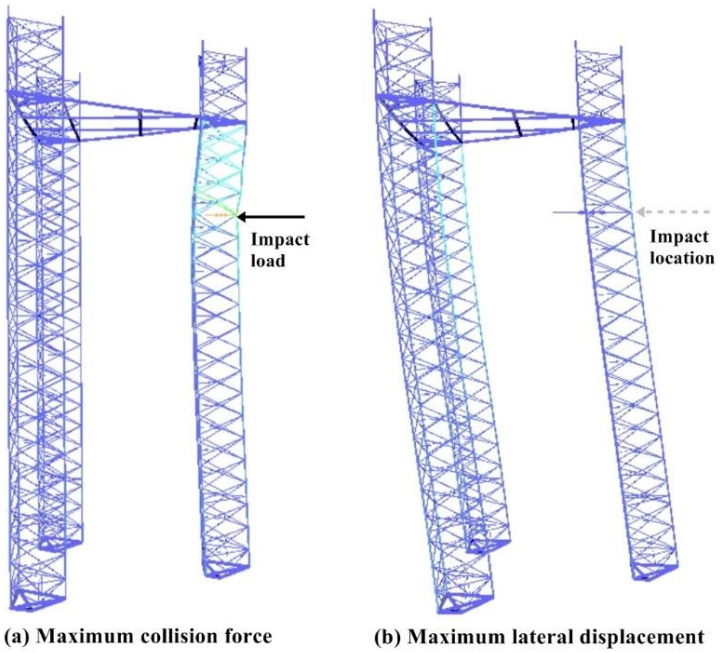

Fig. 11. Snapshots of a dynamic ship-jack up collision analysis at the instant of (a) maximum collision force; (b) maximum lateral displacement (collision force is zero); the picture is reproduced from Amdahl and Eberg (1993).

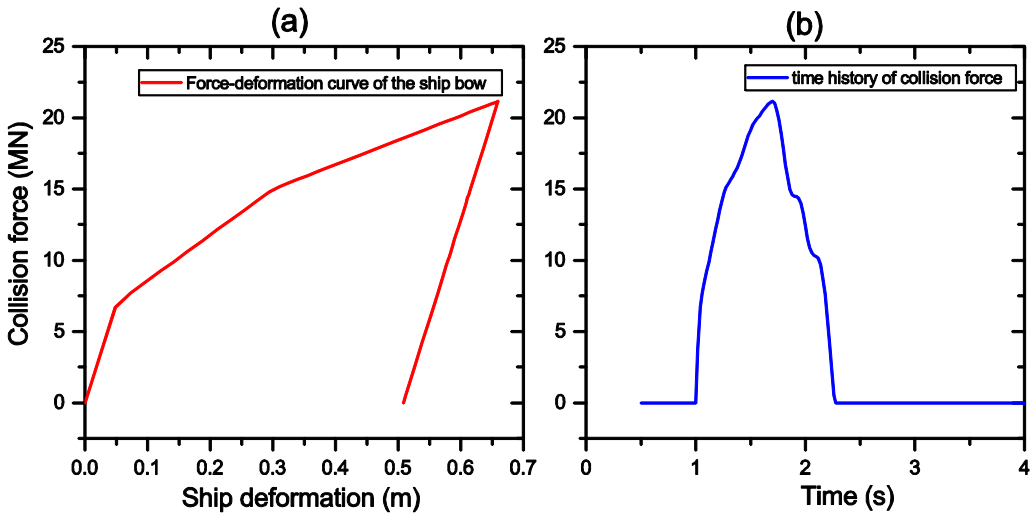

Fig. 12. (a) Force deformation relationship for the ship bow; (b) collision force history

Dynamic effects are more important for 'hard' impacts on legs or joints than impacts on braces. This is because brace impacts are soft and the forces are not sufficient to move the platform substantially, whereas legs or tubular joints have greater strengths. This was confirmed in Azadi (2007), who simulated a ship collision with an 8-leg jacket in the North Sea using USFOS. He also found that the dynamic effects were more significant in broad side collisions than in bow and stern collisions. Levanger et al. (2016) emphasized the dynamic effects in high energy impacts (40 MJ) when carrying out quasi-static and dynamic analyses of a ship-jack up collision using USFOS and ABAQUS. Multiple impacts between a vessel and jack-ups are possible, which

increase plastic energy absorption and damage levels (Ellinas, 1995). Notaro et al. (2015) carried out a nonlinear dynamic analysis of high energy ship-jacket collisions with two methods, i.e. a beam-column analysis using USFOS and the NLFEA method using ABAQUS with shell elements in the impact region and beam elements for the global structure. The two methods obtained reasonable agreement in general, but significant differences may occur for scenarios where local denting or large changes in the contact surface occur. This is because USFOS does not capture the ship-platform interaction effect with increasing contact surface area. Analysts may consider extracting force-penetration curves from the ship impacts on deformable tubular members rather than rigid tubular members as the inputs to USOFS when the ship and platform strengths fall within the shared energy range.

4.3 Platform pile soil interaction

In most cases, it has been observed that the base shears and overturning moments caused by the collision forces are significantly smaller than those created by extreme waves, such that soil failure can normally be disregarded in collisions. The soil will generally contribute little to energy dissipation, and as a first step, it may be useful to model jacket legs as being clamped at the mudline. This simplifies the calculations and is conservative.

Le Sourne et al. (2015) carried out a numerical analysis of an offshore wind turbine jacket impacted by a supply vessel. The soil stiffness was modelled with rotational and translational springs. The results showed that the soil effect had little influence on leg responses. However, the soil effect has often been considered to be important in barge-bridge pier collisions (Consolazio et al., 2003) and bridges under earthquake conditions (Makris and Gazetas, 1992). It is useful to check the capacity of piles in tension/compression and lateral deformation, but it should first be pointed out that neglecting the soil effect is conservative when considering platform safety.

Soil stiffness in ship collisions, if considered, is often modelled with springs. For example, Jin et al. (2005) simplified the effects of soil reactions into three kinds of non-linear springs, namely, a lateral spring representing the lateral bearing capacity of the soil, a vertical spring representing the vertical friction force on the pile surface, and a torsion spring representing the circumferential friction force on the pile surface. Azadi (1998) developed a simplified equivalent model for the pile-soil system, which was modelled as a stack of multiple disks. The idea of a finite disk or strip idealization of the soil medium around a pile was originally introduced by several authors including Nogami and Konagai (1986), Nordal et al. (1985), etc. The disks are connected to each other via pile beam elements. The nonlinear spring and disk representation has been implemented in the USFOS program. The piles and springs can be modelled automatically for each layer based on the API RP2A-WSD (API-RP2A-WSD, 2014) rules. Example pile-soil models are shown in Fig. 13.

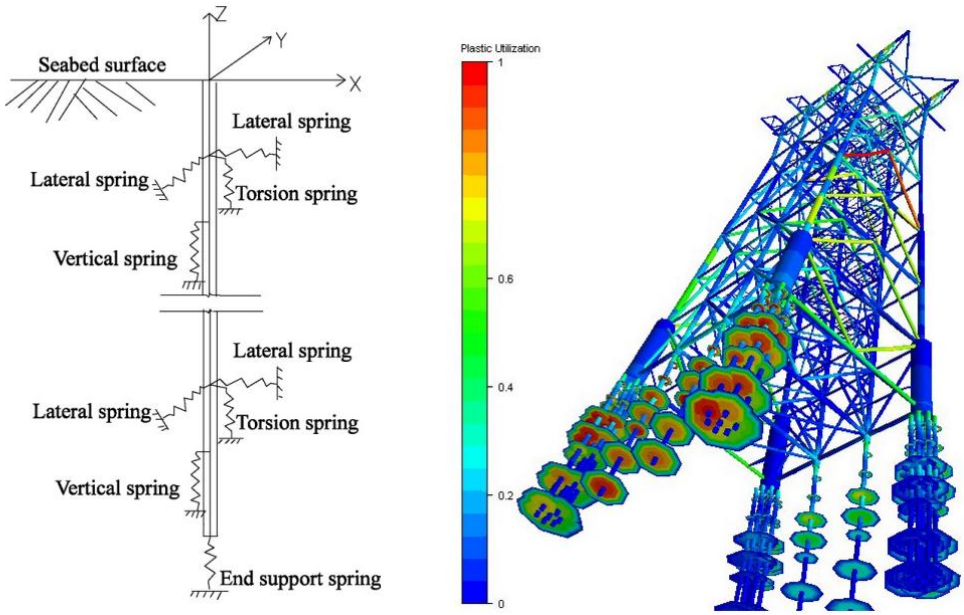

Fig. 13. Pile-soil model with nonlinear springs (left, from Jin et al. (2005)) and disks (right, USFOS examples)

5. Response of tubular members subjected to lateral impacts

Considerable energy will be dissipated through plastic straining of the ship and platform during a collision. Often, braces/legs in direct contact with the ship will deform significantly and absorb a large portion of the total energy. The lateral impact response of a single tubular member involves three deformation patterns of local denting, global bending and membrane deformation. The response behavior can be influenced by many factors such as axial loading, boundary conditions, impact locations, initial inclination angles of tubes, etc.

5.1 Local indentation resistance of tubular members and ring stiffened columns

5.1.1 Local indentation resistance of tubular braces and legs

Many researchers have studied the indentation resistance of tubular members subjected to lateral impacts. Based on experimental observations, they have proposed different idealized models for the deformed tubular cross sections.

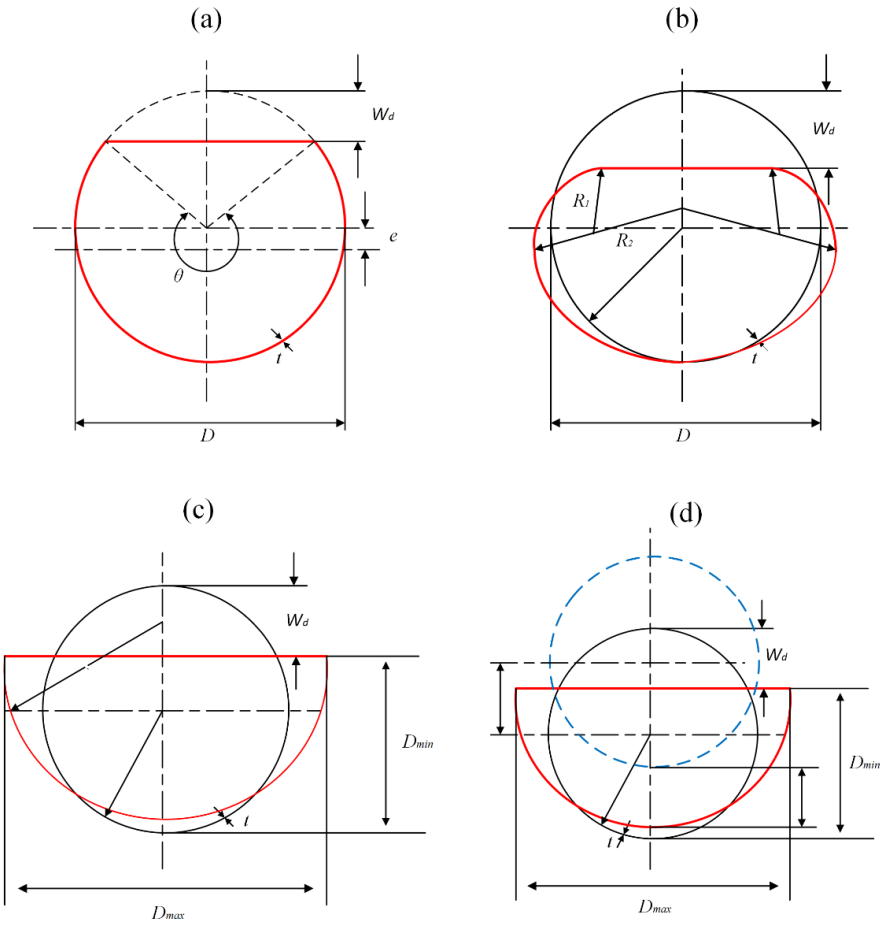

Fig. 14. Idealized damage to tube cross sections during local denting

A few examples are shown in Fig. 14 including:

1) In Fig. 14(a), the dented part is flat and the remaining part is undamaged.

The model in Fig. 14(a) is simple to use and has been employed by many researchers, such as Furnes and Amdahl (1980), Amdahl (1980), Ellinas and Walker (1983) and Allan (1992).

2) In Fig. 14(b), the dented cross section consists of a flat part, and arcs with different diameters in the remaining part.

The model in Fig. 14(b) was proposed by Wierzbicki and Suh (1988) and was also used in Buldgen et al. (2014).

3) Figs. 14 (c) and (d) describe the behaviors of deformed tubular cross sections that include local indentation and combined local denting and global bending. The denting model in Fig. 14 (c) consists of a flat part and an arc with the diameter different from the original.

The model in Figs. 14(c) and (d) was proposed by Jones and Shen (1992). Fig. 14(d) was often used to separate local and global deformations while post-processing experimental and numerical data, such as in Cerik et al. (2016); Travanca and Hao (2014b). More recently, Zhu et al. (2017) carried out an experimental study of the dynamic response of fully clamped pipes subjected to

dropped hammer impacts. They described the cross section of the damaged tube along the tube length with a three-segment mode changing from circular to oval and finally the dented region. The cross section in the dented region was also described using the model in Jones and Shen (1992).

Different formulas for the denting resistance of tubes have been proposed in the literature, the forms of which may vary from empirical to semi-emprical and closed-form solutions. If no extra information is given on the shape of the indenter, the indenter should be considered to be wedge-shaped for a line contact (B=0) and rectangular-shaped for a nonzero contact width B.

Furnes and Amdahl (1980) defined the following relationship between the indenting force *R* and the depth of penetration w_d :

$$R = 15 \cdot \frac{1}{4}\sigma_y t^2 \sqrt{\left(\frac{D}{t}\right)\left(\frac{2w_d}{D}\right)} \tag{2}$$

where σ_y is the material yield stress, *D* is the tube dimeter and *t* is the wall thickness. The model is also adopted in the API RP 2A-WSD (API-RP2A-WSD, 2014) rules.

Amdahl (1980) proposed a local denting model based on a plastic yield line analysis, relating the denting resistance to local indentation. The contact width effect was included by fitting with experimental data. This model uses a flat indenter to represent the ship end or side, and the tube is dented with a flattened top section. The model is adopted in NORSOK N-004, and the denting resistance takes the following form:

$$R/R_c = \left(22 + 1.2\frac{B}{D}\right)\left(\frac{w_d}{D}\right)^{\frac{1.925}{3.5+\frac{B}{D}}} \cdot \sqrt{\frac{4}{3}\left(1 - \frac{1}{4}\left[1 - \frac{N}{N_p}\right]^3\right)} \tag{3}$$

where *B* is the contact width of the indenter. The last term was borrowed from Wierzbicki and Suh (1988) to account for the effect of axial functional loads in the leg. R_c is a characteristic resistance of the tube and is defined as:

$$R_c = \sigma_y \frac{t^2}{4}\sqrt{\frac{D}{t}} \tag{4}$$

Ellinas and Walker (1983) investigated both local denting and global bending deformation of tubular members. The expression for denting resistance of tubes is empirical:

$$R = K \cdot \frac{1}{4}\sigma_y t^2 \cdot \left(\frac{w_d}{D}\right)^{\frac{1}{2}} \tag{5}$$

K is a constant coefficient representing the shape of the indenter, and is normally assumed to be 150 according to experimental observations for concentrated loads.

Wierzbicki and Suh (1988) made the first attempt to derive a closed form solution for the indentation resistance of tubes under combined loading in the form of lateral indentation, bending moment and axial force. The problem was decoupled into the bending and stretching of a series of unconnected rings and generators. The deformed tube sectional shape in Fig. 14 (b) was used. The indentation resistance reads:

$$R = 16\sqrt{\frac{2\pi}{3}\frac{D}{t}\frac{w_d}{D}}\cdot\frac{1}{4}\sigma_y t^2\sqrt{\left(1-\frac{1}{4}\left[1-\frac{N}{N_p}\right]^3\right)} \tag{6}$$

A big advantage of this expression is that it is theoretically derived but still preserves a simple form. According to the formula of Wierzbicki and Suh (1988), a tube's ability to resist local denting depends on tube thickness and material yield stress, but is not related to tube diameter.

Yu and Amdahl (2018) followed the derivation of Wierzbicki and Suh (1988) and extended the model to account for distributed loads with a contact width of *B*. The following equation was obtained:

$$R = 16\left\{\sqrt{\frac{2\pi}{3}\frac{D}{t}\frac{w_d}{D}}\cdot\sqrt{1-\frac{1}{4}\left(1-\frac{N}{N_p}\right)^3}+\frac{B}{D}\right\}\cdot\frac{1}{4}\sigma_y t^2 \tag{7}$$

In a nondimensional format, it reads:

$$\frac{R}{R_c} = 16\left\{\sqrt{\frac{2\pi}{3}\frac{w_d}{D}}\cdot\sqrt{1-\frac{1}{4}\left(1-\frac{N}{N_p}\right)^3}+\frac{B}{D}\sqrt{\frac{t}{D}}\right\} \tag{8}$$

Cho (Cho, 1987, 1990) proposed an empirical equation for denting resistance considering contact width:

$$\frac{R}{m_0} = 2.0\left(\frac{D}{t}\right)^{0.2}\left(\frac{E}{\sigma_y}\right)^{0.5}\left(\frac{w_d}{D}\right)^{0.45}\exp\left\{0.1\left(B/D\right)\left(\frac{w_d}{D}\right)^{-0.3}\right\} \tag{9}$$

where $m_0 = \frac{1}{4}\sigma_y t^2$.

Buldgen et al. (2014) and Jones and Shen (1992) presented analytical solutions for the complete behaviors of tubular members including local denting, global bending and membrane stretching. For local denting, Buldgen et al. (2014) extended the model of Wierzbicki and Suh (1988) to consider different struck tube orientations and positions, and the shape of the striking ship stem. The denting model of Jones and Shen (1992) requires numerical iterations. The expressions are complicated and are omitted here.

The above equations for the indentation resistance of tubes have all been verified to some extent by comparison with experimental results or numerical simulations when they were proposed. The

NORSOK model in Eq. (3) is widely used because it covers the contact width effect. Reasonable accuracy was found in general by Amdahl et al. (2012), Travanca and Hao (2014b) and Watan (2011) etc. Yu and Amdahl (2018) carried out extensive numerical simulations for rigid indenters and deformable ship sterns crushing into tubular members of various dimensions, and verified the denting models against simulation results. They found that the denting models, which considered only concentrated loads, predicted the resistance quite accurately. Detailed comparisons were made especially for the NORSOK model in Eq. (3), the Cho model in Eq. (9) and the modified Wierzbicki and Suh model in Eq. (8) considering the contact width effect in Fig. 15. Results showed that the NORSOK model and the Cho model tended to underestimate resistance for cases with large contact widths, and the underestimation increased with increasing tube wall thickness for the NORSOK model. The modified Wierzbicki and Suh model showed good prediction accuracy for both small and large contact widths.

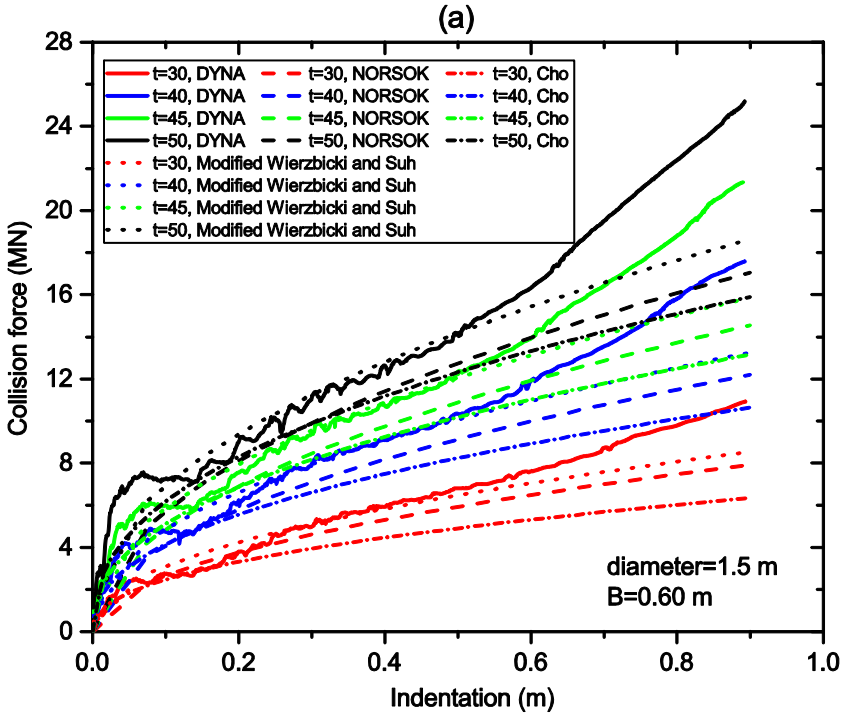

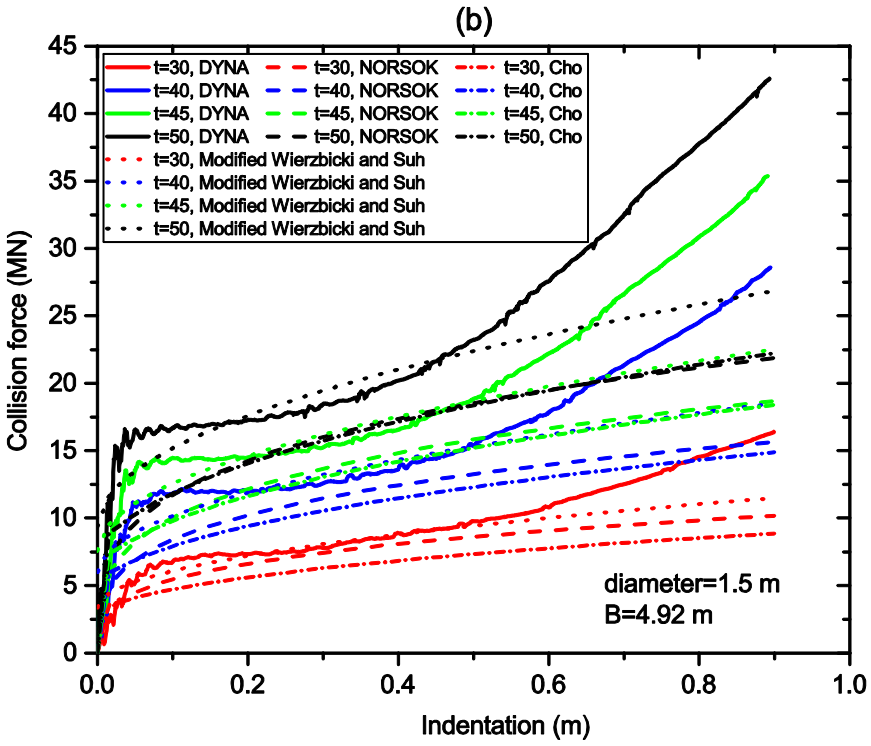

Fig. 15. Denting resistances of tubes impacted by rigid flat indenters with contact widths B= 0.6 m (a) and B=4.92 m (b); the tubes were modelled with lengths of 20 m, diameters of 1.5 m and wall thicknesses varying from 30 mm to 50 mm. A material with a yield stress of 285 MPa was used; from Yu and Amdahl (2018)

More recently, Zhang et al. (2018) carried out a series of drop hammer impact tests on clamped-end tubular members. Three different impact indenter shapes were used, namely wedge shaped, hemispherical and cylindrical indenters. The experiments showed different local deformations in the dented region with different indenters. Unfortunately, a comparison of resistance curves and energy absorption capacities for different indenter shapes was not provided. Based on the experimental data, the authors fitted an equation for the denting resistance of tubular members with increasing indentation depths. The fitted equation is, however, not recommended because the indentation resistance in the equation is linearly proportional to indentation depth and also depends on tube length, which contradicts most previous research and experimental observations.

The shape of damage in the dented zone was theoretically studied by Wierzbicki and Suh (1988), and an expression for the deflection of the leading generator at any location x was obtained:

$$w = w_d \left(1 - x/\xi\right)^2 \tag{10}$$

where, the transverse extension of damage along the tube length ξ is,

$$\xi = \sqrt{\frac{\pi D^2 w_d}{6t}} \tag{11}$$

The obtained shape of the lateral deflection of the leading generator and the shape of the dent correlated well with the experiments by Smith (1982), referring to Fig. 16.

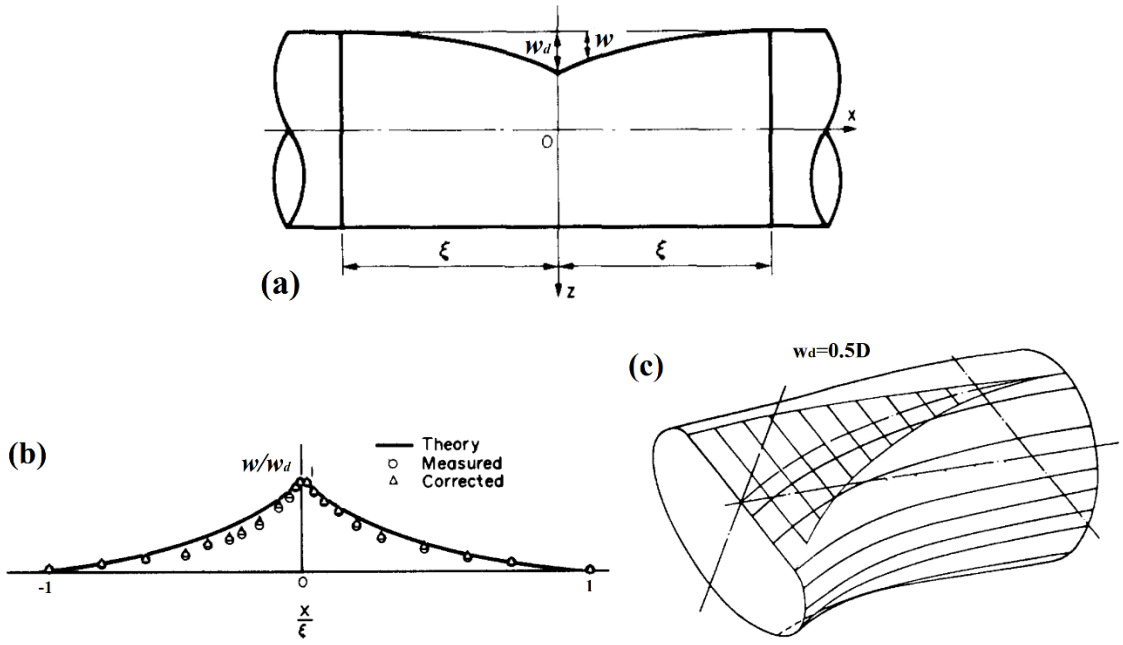

Fig. 16. The development of local damage in the dented zone; from Wierzbicki and Suh (1988)

5.1.2 Local indentation resistance of ring stiffened columns

Ring stiffened columns have large diameter over thickness ratios, and therefore deformation is mainly governed by local indentation. Design equations for ring stiffened columns subjected to collisions have not been officially given in the commonly used design standards. An indication of strength design of large diameter columns against ship impacts is given in the commentary part of DNV RP C204 standard (DNV-GL, 2018), where the design collision force intensity follows a pressure-area relationship similar to that used for ice loads, and the details can be found in Hong et al. (2009) and Storheim and Amdahl (2014). For ductile and shared-energy designs, more investigations are required. Ring stiffened columns are often subjected to local buckling of the shell wall between the rings and in-plane buckling of the rings under external pressure. Design equations to preclude local buckling of ring-stiffened columns are given in the API RP2A-WSD (API-RP2A-WSD, 2014) rules.

Experimental studies on the behavior of ring-stiffened cylinders subjected to lateral indentation were carried out in refs. (Cerik et al., 2015; Harding and Onoufriou, 1995; Karroum et al., 2007a, b; Walker et al., 1987, 1988). A few analytical models have been proposed to predict the resistance to structural indentations for ring stiffened columns. The ring stiffeners are typically treated in two ways:

1) As discrete stiffeners
2) By smearing the stiffener thickness into the attached plate.

Ronalds and Dowling (1987) undertook a plastic analysis of an orthogonally stiffened cylindrical shell with lateral line loading at the mid-span. In the analysis, the shell was assumed

to act as a series of rings and longitudinal beams. The results compared reasonably with their model tests. The formulation, however, yields complicated expressions for design and may also require further validations. Fatt and Wierzbicki (1991) proposed a procedure to calculate indentation resistance of ring stiffened columns. The unstiffened tube was based on the Wierzbicki and Suh (1988) model. The effect of strengthening stiffeners was accounted for using a discrete approach and the smeared method. Cerik et al. (2015) modified the membrane term of the smeared model by Fatt and Wierzbicki (1991) to account for the boundaries of their tests (free to rotate and axially deformable at both ends of ring stiffened columns). The modified formulation predicted the resistance of their results quite well but overestimated the resistance for densely stiffened cylinders when compared with experiments by Harding and Onoufriou (1995). Note that the ring stiffened column models in most of the experiments had short lengths. Hence, after some time, the longitudinal deformation pattern and resistance were influenced by displacements of the boundaries. In reality, ring stiffened columns are quite long, and the propagation of deformations along a column's length is little influenced by the column's boundaries.

The diameters of ring stiffened columns are generally large. In cases of beam and stern end collisions, the assumption of a wide indenter adopted in previous experimental and theoretical studies should be valid (refer to Fig. 17(b)). For ship bow/bulb and stern end impacts, however, the deformations of columns may be concentrated in local regions (refer to Fig. 17 (a)), and the developed analysis models will be optimistic regarding column resistance.

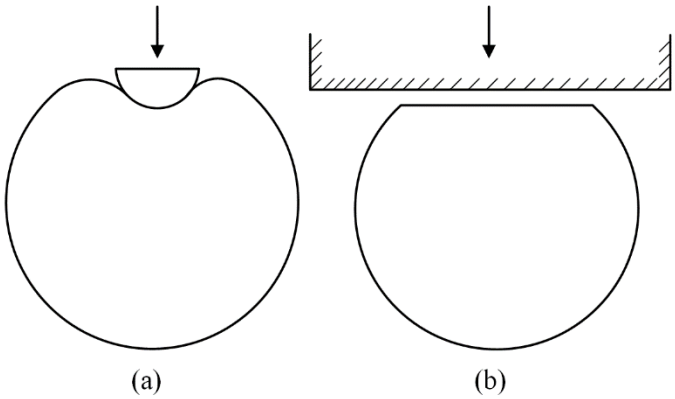

Fig. 17. Cross sections of ring stiffened columns subjected to lateral impact

5.2 Residual bending capacity of dented tubes

A tube with clamped end supports will deform into a three-hinge mechanism when the impact loads exceed the plastic bending collapse load. The maximum lateral load, R_0, can be obtained using the classical plasticity theory and is $R_0 = 8M_p / L$. M_p is the plastic moment capacity of the tube cross section and is $M_p = \sigma_y D^2 t$ for an undamaged thin-walled member. However, the maximum bending capacity often cannot be reached at the cross sections of the ends and the contact region. At the supports, the rear side of the cross section experiences significant compression and may induce local buckling, whereas the front side is subjected to large stretching and may cause fracture. This has been observed in experiments (Amdahl, 1980;

Amdahl, 1983), as shown in Fig. 18. In addition, the shear effect will become important for short beams and will reduce the maximum bending capacity of the cross section at the beam ends; see Jones (2011). In the contact region, local indentation of the tube cross section brings about a reduction in the section modulus and produces an eccentricity about the neutral axis over the damaged region. The combined effect induces a significant loss in load carrying capacity. Considering the deterioration effects at the supports and the contact region, the effective maximum lateral load that a dented tube with clamped supports can carry, is then expressed by

$$R_{0,eff} = \frac{4M_p}{L}(\gamma_1 + \gamma_2) \tag{12}$$

where, γ_1 and γ_2 are the effective bending capacity coefficients of the tube cross sections at the supports and the dented region, respectively as suggested in Foss and Edvardsen (1982). $\gamma_2 = M_{res} / M_p$, and M_{res} is the residual bending capacity of a dented cross section.

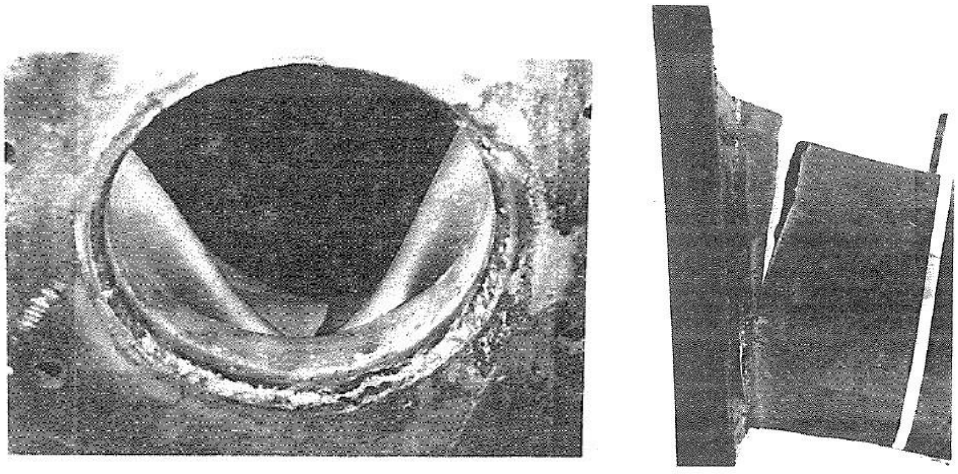

Fig. 18. Local crippling and fracture of a tube cross section at the supports, from Amdahl (1983)

A few models are available from the literature for the bending moment reduction of a dented cross section. The NORSOK N004 standard (NORSOK, 2004) conservatively assumes that the flat part of a dented cross section is non-effective, which yields:

$$\frac{M_{res}}{M_p} = \cos\frac{\theta}{2} - \frac{1}{2}\sin\theta$$
$$\theta = \arccos\left(1 - 2\frac{w_d}{D}\right) \tag{13}$$

Taby (1986) presented a model for the ultimate strengths of dented tubular members subjected to axial compression and bending. It was first assumed that a certain initial longitudinal compressive stress σ_{pd} is needed to obtain initial plastification of the damaged part of the tube's

cross-section. Once σ_{pd} has been exceeded in the damaged fibers, they become ineffective and any additional bending is carried by the remaining effective section. The model was implemented in a program named DENTA and was later adopted in USFOS.

Ellinas and Walker (1983) presented an expression for the residual bending capacity of dented tubes, which partly adopted Taby (1986)'s assumption. The resulting expression yields:

$$\begin{aligned}
&\frac{M_{res}}{M_p} = \cos\beta - \beta \\
&\beta = \sqrt{\frac{w_d}{D}} \cdot \left(1 - \frac{\sigma_{dp}}{\sigma_y}\right) \\
&\sigma_{dp} = \sigma_y \cdot \frac{D}{t}\left(\sqrt{\frac{16}{9}\left(\frac{w_d}{D}\right)^2 + \left(\frac{t}{D}\right)^2} - \frac{4}{3}\frac{w_d}{D}\right)
\end{aligned} \tag{14}$$

Cho et al. (2010) proposed an empirical equation by a regression analysis of results from a series of bending tests with dented tubes at a relatively small scale,

$$\frac{M_{res}}{M_p} = \exp\left[-0.04\left\{\left(\frac{w_d}{D}\right)^{0.7} \cdot D/t\right\} + \left(\frac{B}{D}\right)^{0.1}\right] \tag{15}$$

Buldgen et al. (2014) formulated a moment reduction equation considering the relative positions of the striking ship and the dented tube cross section. Considering a simple right-angle ship collision on a horizontal tube, the expression becomes:

$$\frac{M_{res}}{M_p} = \frac{1}{2}\left(\left(\frac{w_d}{D}\right)^2 - 1\right)\left(\frac{w_d}{D} - 2\right) \tag{16}$$

Jones and Shen (1992) proposed an equation for the development of bending moment with increasing local indentation as:

$$\begin{aligned}
&\frac{w_d}{D} = \frac{1}{2} + \frac{\pi\left[\cos\phi - \cos\left\{\left(\phi + \sin\phi\right)/2\right\}\right]}{2(\phi + \sin\phi)} \\
&\frac{M_{res}}{M_p} = \frac{\pi^2}{2(\phi + \sin\phi)^2} f\left(\phi\right) \\
&f\left(\phi\right) = 2\sin\left(\frac{\phi + \sin\phi}{2}\right) - \sin\phi\left(1 + \cos\phi\right)
\end{aligned} \tag{17}$$

The above models for bending moment reduction due to local denting are compared in Fig. 19. The *D/t* ratio of the tube was set to 30 for the models by Taby (1986), Ellinas and Walker (1983) and Cho et al. (2010), which are *D/t* dependent. Considerable differences appear to exist for

different models. The models by NORSOK standard (NORSOK, 2004) and Ellinas and Walker (1983) predict small values. The NORSOK model is conservative because there is no contribution from the dented part. The expression by Cho et al. (2010) represents pretty well the *mean* strength obtained in tests. The coefficient of variation for *all* dent ranges based on tests of their own and tests by Ueda and Rashed (1985) and Paik and Shin (1989) was estimated to be 8%. For design purposes, it is suggested to use a characteristic strength corresponding to the 5% quantile; this yields approximately 84% of the values plotted in Fig 19, but the values should be larger for small dents.

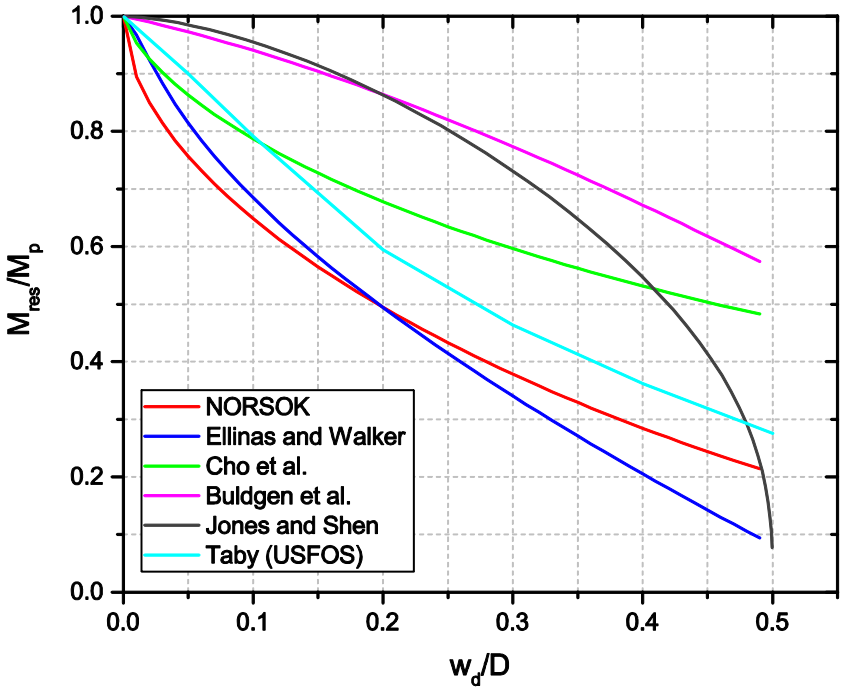

Fig. 19. Bending moment reduction for a dented tube cross section

Taby (1986) checked the bending resistance indirectly through axial compression tests. He obtained excellent agreement with the tests and as such demonstrated the validity of the denting model. The residual strength curves by Cho and Taby confirm each other in the sense that they exhibit the same trends. Thus, for design purposes, the use of the Taby (USFOS) curve seems reasonable. The residual capacities predicted by Buldgen et al. (2014) and Jones and Shen (1992) have a different trend and seem to be too optimistic for the dent range of interest. The situation is somewhat similar to dented offshore pipelines. A review of the residual ultimate strength of offshore pipelines with structural damage can be found in Cai et al. (2017).

5.3 Transition from local denting to global bending

A brace/leg deforms first by local denting in the contact region, and the increasing local indentation continuously decreases the plastic bending collapse load. There exists a transition indentation ratio $w_{d,tran}/D$, beyond which the tube will initiate global bending. Upon further

deformation, the beam plastic resistance may remain constant or increase depending on the tube boundary conditions (see Figs. 20 (a) and (b)). For very thin-walled tubes, the resistance decreases further as denting continues in the beam bending stage.

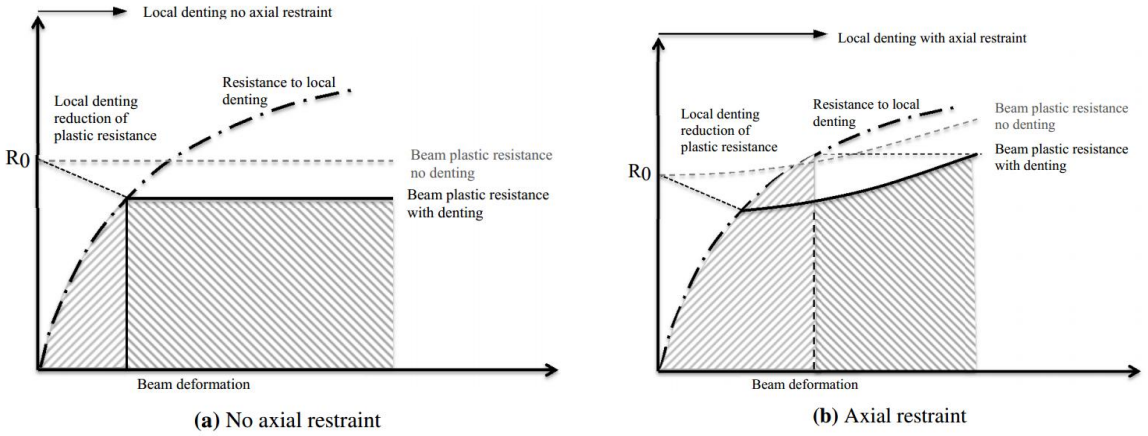

Fig. 20. Plastic resistance vs. beam deformation for varying axial restrain, from Storheim and Amdahl (2014)

de Oliveira et al. (1982) derived the analytical expression for the transition ratio from local denting to global bending as:

$$\frac{w_{d,tran}}{D} = 2(k - \sqrt{k^2 - 1}) \tag{18}$$

where

$$k = 1 + \frac{\pi}{4} \cdot \left(\frac{L}{D}\right)^2 / \left(\frac{D}{t}\right) \tag{19}$$

Ellinas and Walker (1983) gave a more complicated expression for the transition indentation by solving the following equations:

$$\frac{w_{d,tran}}{D} = \left[16/K \cdot \frac{D}{L} \cdot \frac{D}{t}(1 + \cos\beta - \beta)\right]^2 \tag{20}$$

where

$$\beta = \left[1 - \frac{D}{t}\left\{\sqrt{16/9 \cdot \left(\frac{w_{d,tran}}{D}\right)^2 + \left(\frac{t}{D}\right)^2} - 4/3 \cdot \frac{w_{d,tran}}{D}\right\}\right] \cdot \sqrt{\frac{w_{d,tran}}{D}} \tag{21}$$

Yu and Amdahl (2018) proposed an expression for the transition indentation ratio considering the effect of distributed loads over a contact length of B. The transition indentation ratio is obtained by solving:

$$\frac{R_0}{2R_c}\left(1+\sqrt{1-\frac{w_{d,tran}}{D}}-\sqrt{\frac{w_{d,tran}}{D}-\left(\frac{w_{d,tran}}{D}\right)^2}\right)=\left(22+1.2\frac{B}{D}\right)\left(\frac{w_{d,tran}}{D}\right)^{\frac{1.925}{3.5+\frac{B}{D}}} \quad (22)$$

where

$$R_0 / R_c = 32\sqrt{\frac{D}{t}}\cdot\frac{D}{L-B} \quad (23)$$

Yu and Amdahl (2018) found that the rear side of the struck tube would contract during local denting due to ovalization of tube cross sections; see Fig. 14(c), and the nodal velocity at the rear side would thus not continuously increase. This made it easier to separate the denting and bending stages. They verified the analytical expressions for the transition ratio using numerical results and good agreement was obtained in general for the three models.

The transition indentation ratio $w_{d,tran}/D$ depends on R_0/R_c according to the models by de Oliveira et al. (1982) and Yu and Amdahl (2018). R_0/R_c varies with powers of 3/2, -1/2 and -1 for the diameter, thickness and length of a brace/leg, respectively. Another important factor is the contact width *B*. On one hand, it reduces the effective length when calculating R_0 and therefore yields a larger R_0/R_c and subsequently a larger $w_{d,tran}/D$; on the other hand, the capability to resist local denting is enhanced with increasing contact width, which reduces the $w_{d,tran}/D$. The decreasing tendency seems to be dominant with increasing contact widths.

Fig. 21 shows the variations in transition indentation ratios over wide ranges of L/D and D/t by using de Oliveira et al. (1982)'s model. L/D was varied from 5 to 60 and D/t from 10 to 80. It was found that the large transition indentation ratios concentrated in the region with small L/D and large D/t values. According to the numerical simulation results in Yu and Amdahl (2018), there exists a threshold value of the $w_{d,tran}/D$, below which almost no local denting occurs before bending. A threshold value of 0.15 was recommended by Yu and Amdahl (2018).

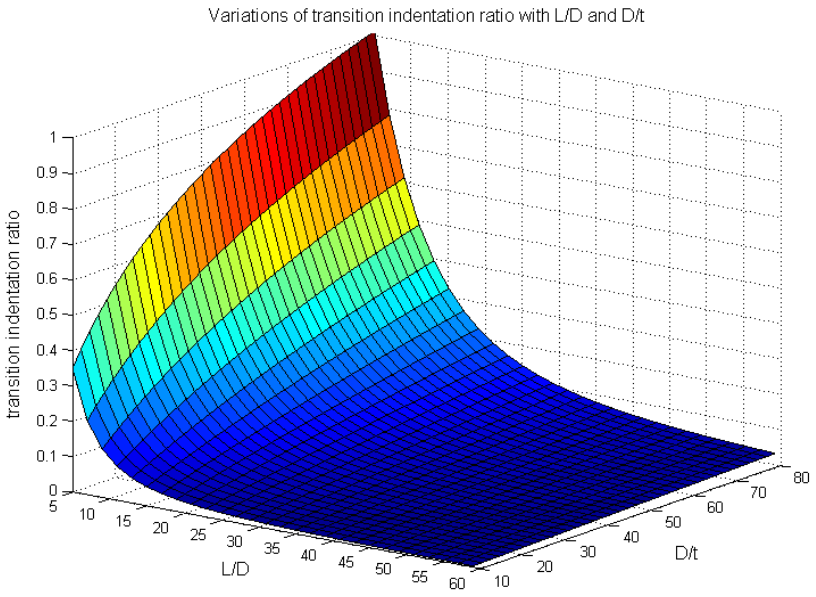

Fig. 21. Variations in the transition indentation ratios with L/D and D/t

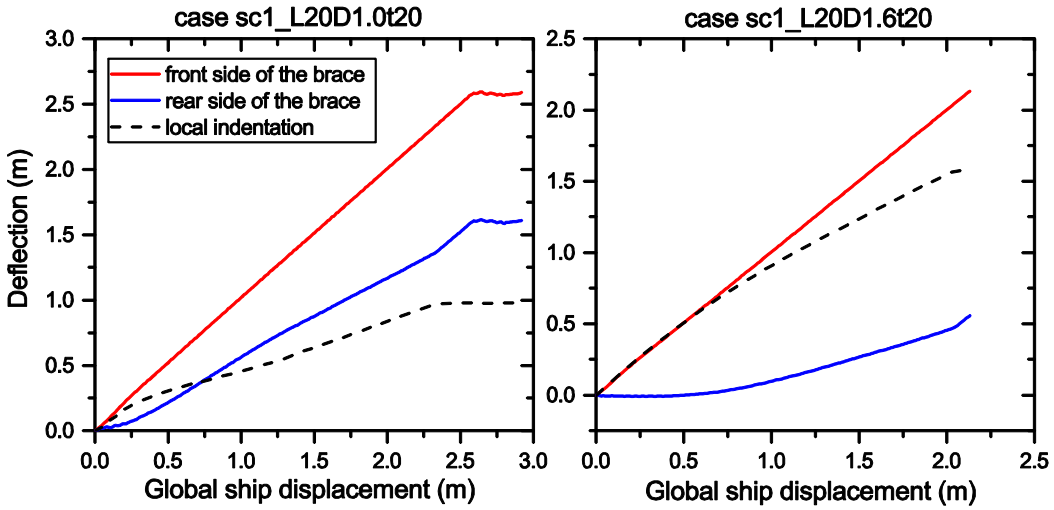

Fig. 22. Indentation and nodal displacements on the front and rear sides of tubes with dimensions of (left) L=20 m, D=1.0 m and t=20 mm; (right) L=20 m, D=1.6 m and t=20 mm when impacted by a supply vessel stern; from Yu and Amdahl (2018)

The concept of transition ratio aids in understanding the dominant deformation patterns (local denting, bending or combined denting and bending) given certain tube dimensions. Global bending commences once the transition indentation is reached, but this does not mean local denting will cease immediately. Fig. 22 shows the nodal displacements on the front and rear sides of a tube, from which local denting may still increase after initiation of global deflections. It is therefore not a good criterion to keep a tube cross section compact by limiting the transition ratio to a small value.

5.4 Bending and membrane stretching of tubes

Tubes will start global bending and deflect laterally when the transition indentation is reached. For tubes with clamped boundaries, membrane force increases with increasing lateral deflections and later becomes dominant up to fracture if the adjacent members and joints have sufficient strengths against being pulled in.

Based on a rigid-plastic analysis, Guedes Soares and Søreide (1983) presented an analytical model for the resistance of laterally loaded tubular members. Local indentation is assumed to be small and negligible. The interaction effect of bending moment and axial force is considered. For a perfect tubular cross section, the interaction function yields:

$$\frac{M}{M_p} - \cos\left(\frac{\pi}{2}\frac{N}{N_p}\right) = 0 \tag{24}$$

where M_p is the plastic bending moment of the cross section, and N_p is the plastic yielding force of the cross section in tension.

The following expression for the resistance-deflection relationship is obtained:

$$\frac{R}{R_0} = \begin{cases} \sqrt{\left(1-\left(\frac{w_b}{D}\right)^2\right)} + \frac{w_b}{D}\arcsin\left(\frac{w_b}{D}\right); & \frac{w_b}{D} \le 1 \\ \frac{\pi}{2}\frac{w_b}{D} \qquad\qquad\qquad\qquad\quad ; & \frac{w_b}{D} > 1 \end{cases} \tag{25}$$

where w_b is the lateral deflection of the beam. This model shows very good agreement for minor denting cases, but the difference becomes large with increasing local indentations.

De Oliveria (1981) presented a beam deformation model for tubes considering the axial and rotational flexibilities at the supports. The interaction between bending moment and axial membrane forces was accounted for, and local indentation was neglected. The results showed that the axial stiffness at the supports was very important for the development of membrane forces in the tubes, especially for cases with large lateral transverse displacements. The influence of finite axial stiffness is also included analytically in the updated DNV RP C204 standard (DNV-GL, 2018), where the expressions (slightly simplified) for the lateral deflection resistance of tubular members with finite axial stiffness and fixed rotations at the supports yield:

$$\frac{R}{R_0} = \begin{cases} 1-\left(\frac{N}{N_p}\right)^{\frac{\pi}{2}} + \frac{\pi}{2}\left(\frac{N}{N_p}\right)\left(\frac{w_b}{D}\right); & \frac{N}{N_p} \le 1 \\ \frac{\pi}{2}\frac{w_b}{D} \qquad\qquad\qquad\qquad\quad ; & \frac{N}{N_p} > 1 \end{cases} \tag{26}$$

where the development of axial forces with lateral deflections is:

$$\frac{N}{N_p} = \frac{w_b}{D} - \frac{1}{c}\left(1 - e^{-c\cdot\frac{w_b}{D}}\right); \quad \frac{N}{N_p} \le 1 \tag{27}$$

c is the non-dimensional spring stiffness

The effect of rotational stiffness should be small in practice and is limited by plastic bending moment. The bending moment tends to become insignificant at large deformations when the membrane force dominates.

The above expressions are based on perfect tubular cross sections neglecting local denting. It should be noted that for braces supported by strong tubular joints and adjacent structures, the effect of local indentation becomes negligible when axial membrane force dominates, and the resistance will finally converge to the solution with perfect cross sections in pure tension. For legs, local indentation can be substantial, whereas the development of axial membrane forces compared to the yield axial force is limited. It may be useful to assume constant forces in the beam bending stage; see Fig. 21(a).

A few researchers have proposed analytical solutions for the lateral deflection resistance of tubular members considering a dented cross section, such as Ellinas and Walker (1983), Jones and Shen (1992), Buldgen et al. (2014), etc. Ellinas and Walker (1983) assumed that local denting ceased immediately when the tube started global bending. The ultimate lateral load was reached when the tube started global bending and the force was kept constant afterwards by neglecting the development of membrane forces. Jones and Shen (1992) considered three deformation stages of local denting, global bending and membrane stretching, and allowed local denting deformations to continue in the global deformation phase. The resulting expressions are however complicated for design purposes. Generally good agreement was obtained with the maximum permanent transverse displacements from experimental tests in Jones et al. (1992), in which results from a series of static and dynamic impacts for tubes with various dimensions were reported. They found that regardless of whether bending or local denting governed the tube deformation, the dimensionless dissipated strain energy changed almost linearly with the maximum permanent transverse displacement. Similar findings were reported by Travanca and Hao (2014b) through extensive numerical simulations. Buldgen et al. (2014) presented an analytical solution considering the complete behaviors including local denting, global bending and membrane stretching. The different orientations and positions of the struck tube, and the shape of the striking ship stem were accounted for. The proposed method was verified to be of reasonable accuracy using finite element software LS-DYNA. It is not clear whether it is important to consider tube orientation and stem shape, but accounting for the two factors makes the expressions rather complicated.

Le Sourne et al. (2015) carried out a numerical analysis of an offshore wind turbine jacket impacted by a supply vessel, and found that for the leg impact case, the impacted leg dissipated approximately 60% of the total internal energy, some plastic strains also developed in the legs extremities and the rear leg could be punched by the connected braces. It is therefore not a good approximation to assume that all the energy is dissipated through deformations of the impacted leg. Based on the observations, Le Sourne et al. (2016) derived analytical expressions for energy

absorption in two additional scenarios other than that wherein the impacted leg was laterally deformed. The first considered a leg punched by one or several compressed braces and the second considered the buckling of a rear compressed leg near the mudline during the overall deformation of the jacket. Based on the concept of the super element method, they proposed an efficient method that included simplified solutions for local denting, global bending, axial stretching, brace punching and buckling. The proposed method was verified to be of reasonable accuracy with a few cases using LS-DYNA for the same wind turbine jacket, from which they obtained the idealized displacement fields. The transferability to other platforms needs further investigations. Another concern with respect to the work is that application of simplified methods to regions far away from the impacted location may not be safe for structural design because many uncertainties are not captured by the idealized model, such as fracture and failure and force redistribution throughout the entire structure after member failure.

Tubular pipes, containing liquid, gas or granular materials that are often pressuried, have similar structural performances when subjected to lateral impacts. The material contents in pipes will provide inertia resistance to deformation through the added mass effect, and the effect increases with increasing density of the contents. Jones and Birch (2010) showed that increasing internal pressure caused a small reduction in the maximum permanent transverse displacement but caused an important reduction in impact energy for failure. More research on the lateral impacts of matter filled pipes can be found in refs. (Jones and Birch, 1996; Ma and Stronge, 1985; Nishida and Tanaka, 2006; Palmer et al., 2006).

5.5 Influence of axial pre-compression and boundary conditions

Tubular members, especially platform legs, are often preloaded to some extent by carrying the weight of the platform and additional environmental loads. The effect of axial pre-compression is two-fold; i). The axial force will reduce the plastic bending moment of the cross-section and the denting resistance. ii) During finite lateral deformation it will create additional bending moments. It is noticed that in many cases the axial stress is small compared to the yield strength such that the first effect is small. Furthermore, many platforms possess significant redistribution capabilities so that the axial force in a leg is reduced when the leg deforms. This can be well illustrated by Fig. 23, in which an offshore jacket was impacted by a vessel on the leg. Both static and dynamic analyses were carried out using USFOS. The static analysis in Fig. 23 (a) shows that a buckled brace fairly distant from the contact region can cause force redistribution throughout the entire platform, and can be important in resisting collision loads. The dynamic analysis results from Fig. 23 (b) by Skallerud and Amdahl (2002) showed that the plastic deformation of the leg caused the axial force in the leg to unload its share of the topside weight; in the extreme, it became tensile. By simple equilibrium, the opposite leg had to unload. The net result was that the two central legs had to carry the entire weight of the platform. Most investigators have studied the behaviors of tubular members with constant preloads, thus implicitly assuming a non-redundant structure.

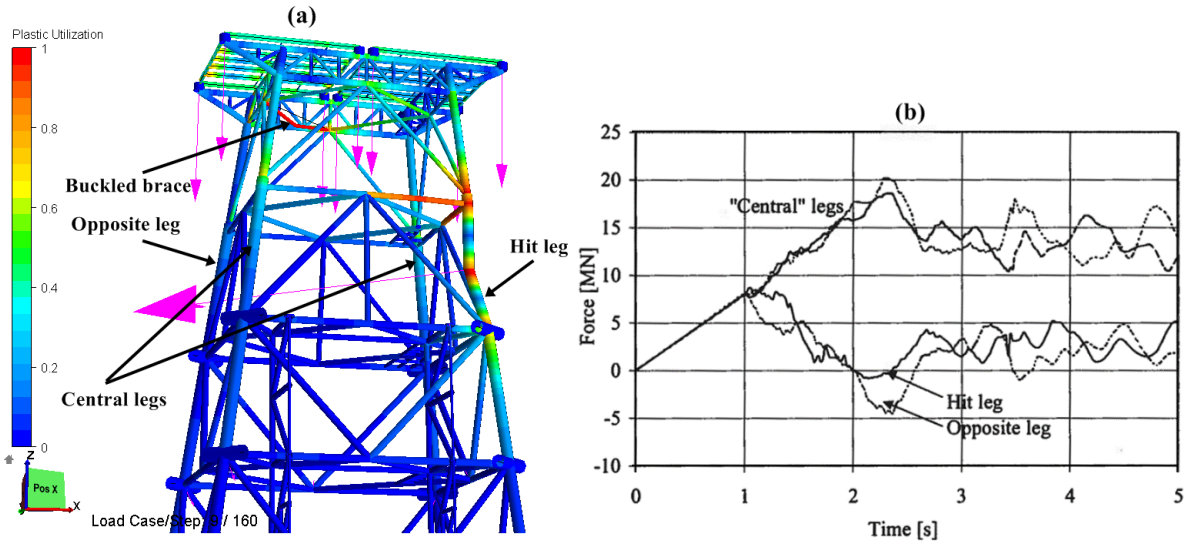

Fig. 23. (a): Jacket subjected to a leg impact from a static analysis; (b): axial forces in leg collisions from a dynamic analysis, from Skallerud and Amdahl (2002)

Wierzbicki and Suh (1988) presented a closed form solution for the indentation resistance of tubes under combined axial forces and bending moment as shown in Eq. (6). The last term represents the degradation effect of the load carrying capacity of preloaded tubes. The theory predicted a threshold force ratio of N/N_p=-0.5874 (N_p is the ultimate strength of the tube in tension), below which no lateral forces can be equilibrated by the system. NORSOK N004 (NORSOK, 2004) considered the strength reduction due to axial compression loading by introducing an effective factor *k*:

$$k = \begin{cases} 1.0; & \dfrac{N_{Sd}}{N_{Rd}} \le 0.2 \\ 1.0 - 2\left(\dfrac{N_{Sd}}{N_{Rd}} - 0.2\right); & 0.2 < \dfrac{N_{Sd}}{N_{Rd}} < 0.6 \\ 0; & \dfrac{N_{Sd}}{N_{Rd}} \ge 0.6 \end{cases} \tag{28}$$

where N_{Sd} and N_{Rd} are the design axial compressive force and resistance, respectively.

In order for the above equations to be valid, no local buckling of the tube cross section shall occur. Local buckling of unstiffened tubular cross sections can be checked according to the API rule (API-RP2A-WSD, 2014) and DNV-GL RP C204 (DNV-GL, 2018) standard. Both rules indicate significant dependence on the diameter over thickness ratio (D/t). The API rule (API-RP2A-WSD, 2014) requires that unstiffened cylindrical members with D/t greater than 60 should be investigated for elastic and inelastic local buckling of cross sections under axial compression.

By means of finite element analyses, Khedmati and Nazari (2012) preloaded tubes to force levels of 0% to 100% of the yield strength, and found that the compressive loads significantly degraded the ultimate strength and energy absorption capabilities of the tubes. The ultimate strength of

tubular members was found to increase when the impact position moved from the middle towards the end. However, the tubes tend to fracture early and absorb less energy as shown in the experiments by Jones et al. (1992). The effect of preloading was also studied experimentally and numerically in Zeinoddini et al. (Zeinoddini et al., 1998, 1999; Zeinoddini et al., 2008; Zeinoddini et al., 2002). Numerical and experimental results from Khedmati and Nazari (2012), and Zeinoddini et al. (Zeinoddini et al., 1998, 1999; Zeinoddini et al., 2008; Zeinoddini et al., 2002) indicated that, contrary to the theory predicted by Wierzbicki and Suh (1988), a member with an axial compressive preloading exceeding $0.5874N_p$ could still resist some lateral load. The reason may be that the equation proposed by Wierzbicki and Suh (1988) was obtained by assuming no global rotation in the member, which is questionable for the real behavior of a tube (Zeinoddini et al., 1998).

The effects of three different boundaries conditions at the supports were investigated by numerical simulation in Khedmati and Nazari (2012) and Zeinoddini et al. (1998). The considered boundary conditions were type 1 with free axial sliding and rotation, type 2 with free sliding and fixed rotation, and type 3 with fixed sliding and rotation. Typical resistance-displacement curves are shown in Fig. 24. The resistances of tubes under type 1 and 2 conditions have clear maximum values, and the governing deformation modes are local denting and beam bending. For type 3, the resistance increases continuously with lateral deflections due to significant membrane forces.

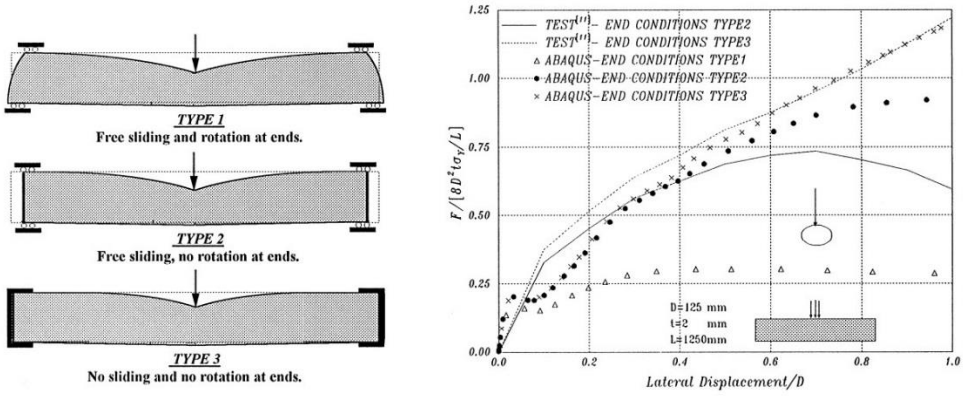

Fig. 24. Numerical and experimental (Søreide and Kavlie (1985)) load displacement curves for tubes with different types of end conditions, from Zeinoddini et al. (1998)

However, none of the above three types of boundary conditions provide a good representation of the boundaries of braces and legs in real platforms. A more realistic representation of the boundary conditions may be to assume finite axial and rotational stiffnesses at the supports. The axial stiffness governs the development of membrane forces and influences the total resistance significantly. Qvale (2012) and Watan (2011) considered the axial stiffness of jacket legs when analyzing supply vessel side and stern collisions with jacket platforms. They removed the struck leg from the platform in USFOS and applied axial forces at the end nodes (see Fig. 25 (a)). The axial stiffness was taken as the tangent of the obtained force-displacement curve and then implemented in the LS-DYNA model as the spring stiffness (see Fig. 25 (b)). Results showed that the force decreased when considering axial flexibilities compared to that under clamped end

conditions. The reduction was especially significant for weak columns because they experienced large deformations. Rotational springs are needed for better representation of the boundaries. A more accurate way to represent the boundary conditions of a member may be to properly model the tubular joints and adjacent tubular members.

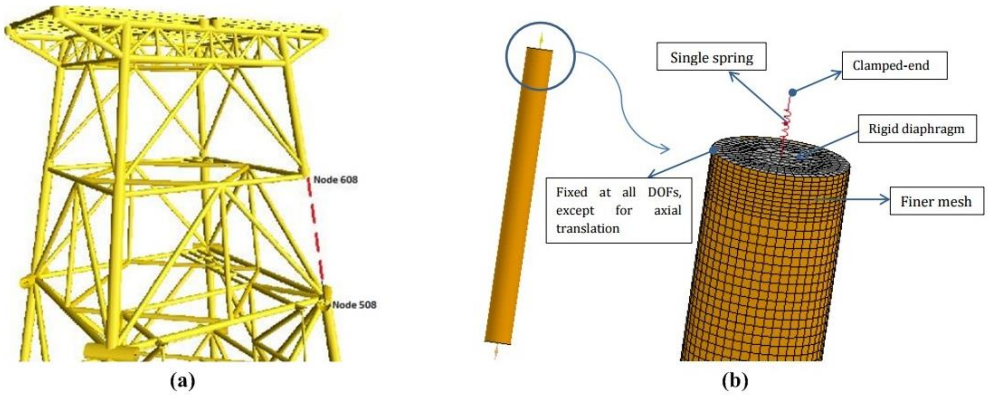

Fig. 25. Numerical simulation of ship collisions with jacket legs considering axial flexibilities, from Qvale (2012) and Watan (2011)

6. Responses of tubular members subjected to axial compression

Supporting braces can be loaded axially during collisions, especially when a ship collides onto a platform tubular joint; e.g., Wang et al. (2016). Responses of circular tubes under compression have been investigated by many researchers, especially as energy absorbers in the automobile industry. A few review articles on thin-walled structures as energy absorbers can be found in refs. (Abramowicz, 2003; Alghamdi, 2001; Olabi et al., 2007).

A series of experiments was carried out on steel and aluminum tubes of different dimensions that were loaded quasi-statically and dynamically, such as Guillow et al. (2001), Karagiozova and Jones (2008), Andrews et al. (1983) and Abramowicz and Jones (1997). Depending on tube dimensions, boundary conditions, and impact velocities, circular tubes behave quite differently. Fig. 26 shows three main deformation patterns from experiments: the axisymmetric mode (also known as concertina mode), the asymmetric mode (also called diamond mode), and the global bending mode due to Euler buckling. Some tubes may exhibit combined deformation modes.

Andrews et al. (1983) summarized the experimental results and presented a classification chart of the deformation modes of quasi-statically compressed aluminum alloy tubes; see Fig. 27. Similar charts can also be found in Guillow et al. (2001). The experiments showed that the initial buckling phase is decisive in forming the energy absorption mechanisms. A static critical tube length, L_{cr}^{static}, exists for a particular diameter over thickness ratio D/t, such that tubes shorter than that length collapse progressively, whereas longer tubes develop a global bending mode. In general, tubes used in offshore jacket and jack-up platforms have large length over diameter ratios L/D, and deform mainly in the global bending mode. Abramowicz and Jones (1997) and Karagiozova and Alves (2004) showed that the critical length for buckling transition increased when the tubes were loaded dynamically. This was attributed to the increased lateral inertia of the

shell. However, in ship-platform collisions, impact velocities are generally low, and the dynamic effects are secondary. Foss and Edvardsen (1982) compared the energy absorption capabilities of offshore tubular members subjected to lateral impacts and axial compression considering different boundary conditions. The test results showed that a compression member absorbed energy similar to that for a bending member and may be treated as a bending member for energy absorption purposes.

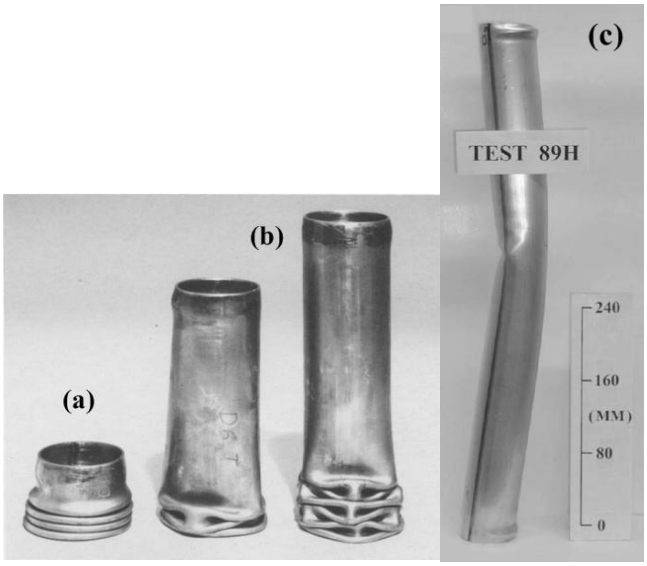

Fig. 26. Deformation of tubes subjected to axial loading (a) axisymmetric mode, (b) asymmetric mode, (c) Euler buckling, from Abramowicz and Jones (1986) and Guillow et al. (2001)

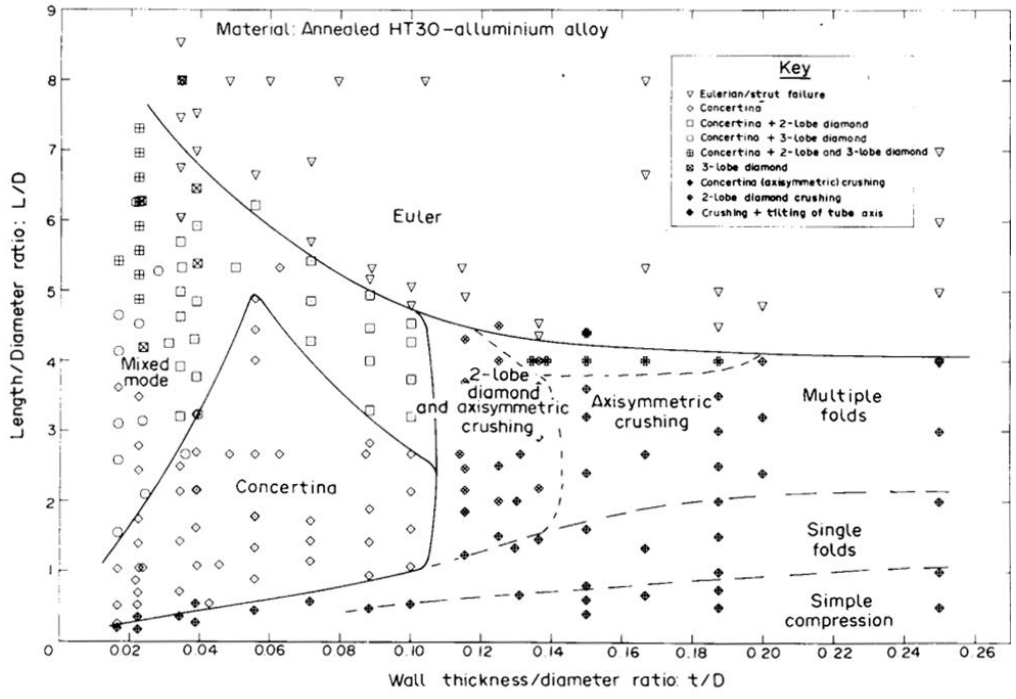

Fig. 27. Classification chart for deformation modes of aluminum alloy tubes; from Andrews et al. (1983)

Large diameter thin-walled cylinders are also commonly used as compression elements in offshore installations such as semi-submersibles, spars and more recently as buoyancy columns for floating offshore wind turbine foundations. They are often stiffened with ring stiffeners and/or stringers. For such members, progressive buckling modes may develop. Analytical solutions for the average collapse load of the axisymmetric and asymmetric models in Fig. 26 have been provided by Alexander (1960) and Johnson et al. (1977), respectively. Amdahl and Søreide (1981) studied the axial crushing of a cylindrical bulbous bow stiffened with transverse frames, longitudinal stringers and a centerline bulkhead. The method proposed by Gerard (1958) that cuts cross sections into simple elements was found to agree well with experimental curves. Further discussion is omitted.

7. Behavior of tubular joints

The integrity of tubular joints is crucial to ensure the smooth transfer of the collision forces from the impact location to the adjacent structures. In the initial stages, the hit brace or leg deforms by bending, whereas braces may develop significant axial tension forces during finite deformations. In addition, legs may sometimes be capable of completely unloading the axial compressions induced by the functional loads and develop some tension, but the tension forces will be small compared to the yield forces.

The ultimate load carrying capacities of tubular joints determine to a large extent the amounts of energy absorbed by bracing members. Failure of tubular joints may be caused by buckling of the chord, excessive deformations, or the initiation and propagation of cracks. The capacities of tubular joints are typically expressed in code requirements for offshore structures, e.g., ISO 19902 (ISO, 2007), API RP 2A-WSD (API-RP2A-WSD, 2014) and NORSOK N004 (NORSOK, 2004). Three characteristic actions are often considered: compression or tension, in-plane bending (IPB) and out-of-plane bending (OPB). Normally OPB predominates for impact actions. Combined axial force, IPB and OPB are considered through interaction formulas. The effect of axial force in the chord (i.e. the leg) is also taken into account. It is distinguished by three different joint categories: X-, K- and T-joints. The classification depends on the load transfer. The behavior of X-, K- and T-joints up to peak capacity is given as a nonlinear force-displacement/moment-rotation curve according to the formulations developed in Joint Industry Projects carried out by MSL Engineering Ltd. (MSL Engineering Ltd, 1996, 2000) considering also the tension ductility limits. The actual behavior of tubular joints may be a combination of the three load categories, and the contribution from each category may vary during the impact. Hence, the joint may need to be constantly reclassified during the collision action. This approach is adopted in USFOS.

It is noted that joint classification and resistance are based on the plane of action, neglecting the effect of out-of-plane braces. The approach is considered to be conservative for multi-planar joints. This circumstance and the fact that capacity formulas are based on characteristic resistances make it likely that the use of shell element modeling of joints in a nonlinear finite element analysis of a ship impact will yield larger joint capacities than those given in the design codes.

A collision analysis based on shell finite element modeling of a joint and braces framing into the joint of a jacket was carried by Notaro et al. (2015) using ABAQUS explicit. The colliding object was assumed to be the pontoon bow of a semi-submersible platform. The pontoon bow was also modeled with shell finite elements, which allowed a significantly better simulation of the contact area and dent growth. The investigation confirmed a somewhat higher resistance of the T-joint in the FE analysis compared to the USFOS use of code formulations. The multi-planar effect was probably low in the present case because of the simple joint geometry and only two out-of-plane braces. Notaro et al. (2015) also simulated a direct hit on a joint that induced local denting of the chord wall. The simple local denting formulations used in the beam models are not intended to include chord walls in tubular joints; the damage obtained in the FE analysis was smaller, but in the same order of magnitude. Part of the difference was also attributed to more realistic development of the contact area and dent in the FE simulations.

8. Ultimate strength of damaged tubes

Depending on impact intensity and tube strength, tubular members will absorb impact energy by developing deformations of the following forms:

1. Local denting of the tube wall without overall bending of the member
2. Overall bending without denting of the tube wall
3. Combined overall bending and denting deformations

The damage types seem to be governed by the transition ratio as discussed in *Section 5.3*. The damaged tubular members may be subjected to various loading conditions during platform operations, which may include axial compression, bending, combined axial compression and bending, and combined axial compression and hydrostatic pressure.

A series of axial compression tests of damaged tubes both at a small scale and at full scale was carried out by Smith et al. (Smith et al., 1979; Smith et al., 1980; Smith et al., 1981). The results indicated that the small-scale experiments provided satisfactory accuracy when compared to the full-scale tests. The ultimate strength of the slightly damaged members was significantly less than that of the undamaged ones. For tubes with only overall bending damage, an elastoplastic beam column analysis (Smith et al., 1979) showed good correlation with test results. For tubes with local indentations, they proposed a semi-empirical method based on the experiments by introducing an effective modulus and yield stress in the dented region.

Taby et al. (1981), Taby and Moan (1985) and Yao et al. (1988) proposed an analytical-numerical model of a damaged tubular member subjected to axial compression based on yield line theory. The theory was later adopted in USFOS. The tubes were loaded incrementally. After initial plastification, the dented region was assumed to be ineffective and an additional load increase was carried by the elastoplastic behavior of the undamaged part of the dented cross section. Plastic hinges were introduced when the ultimate strength was reached. The incremental load-deformation relationship in the post ultimate stage was formulated in the form of stiffness matrices. The interaction between bending moment and axial forces was considered, where the dent was in compression. A series of axial compression tests on damaged tubes was carried out in 1980 and 1983, and was reported in Taby and Moan (1985) and Taby (1986). The experimental

results showed that dent depth increased significantly in the post-ultimate stage and the force dropped rapidly, see Fig. 28. An empirical function was derived to account for the growth in dent depth. After calibration, the model compared reasonably well with the experiments.

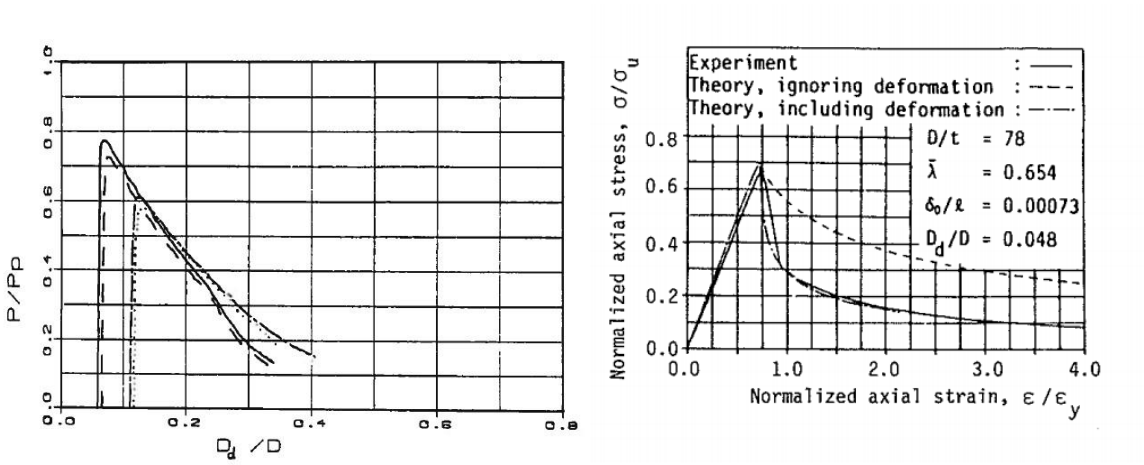

Fig. 28. (left) Growth of dent depth as a function of axial load; (right) axial load versus axial shortening; from Taby (1986)

Considering the general loading case, the resultant bending moment of the dented cross section may have an arbitrary angle with respect to the dent. This was considered in Ueda and Rashed (1985). They derived an ultimate strength interaction relationship of a dented tube member subjected to axial force and bending moment in two perpendicular directions. A series of bending tests of dented tubes was carried out. The results showed that the effect of a dent on the ultimate strength reduction was predominant when the dent was in compression. The effect was less when the dent was in tension or at the neutral axis. The predicted results agreed reasonably well with the experiments.

Ellinas (1984) presented a simple method for estimating the reserved strength of damaged tubes with local denting damage, overall beam deflection, and combined local denting and overall deflection damage. The method showed a clear lower bound when compared to previous experiments and was conservative for safety considerations. A parametric study was carried out and showed that the behavior of damaged tubular members was highly influenced by the column slenderness parameter λ_R, the dent depth and the overall bending imperfection. The ultimate strength reduction caused by initial local denting damage was potentially more important for cases with small λ_R and small bending imperfections.

Unlike the previous analytical models assuming ineffectiveness of the dented region after initial plastification, Durkin (1987) represented fibers inside the dents as a series of longitudinal strips with a deflection shape that was characteristic of a beam on an elastic foundation. Combined axial loading and bending moments were assumed. The ultimate strength was reached when a point of plastic instability occurred during iterations and the stress level was maximized. The predicted results of the models were compared with experiments and numerical simulations, and the differences of the ultimate strength values were reported to be within 5%. The behavior of dented tubular members with and without considering local buckling and residual stresses was

also analyzed by Duan et al. (Duan et al., 1993; Duan et al., 1990) using an empirical-analytical moment curvature approach.

The effect of residual stress in the dented region is often considered to be negligible in the analytical models. Pacheco and Durkin (1988) carried out experimental and numerical studies on the behavior of dented tubular members and showed that the exclusion of the residual stress effect will lead to small underestimations of residual strength. The underestimation was likely to be substantial for tubes with large dents.

9. Design considerations

9.1 The design philosophy

A crashworthy structure against ship impacts implies a structure that is designed such that it is capable of withstanding collisions without global collapse. The energy may be absorbed either by plastic straining of the structure itself or by deforming the striking ship. According to DNV-RP-C204 (2010), when designing offshore structures against accidental ship impacts, significant structural deformations may be allowed provided that the damage does not lead to progressive collapse of the structures or destroy the usability of escape ways. The platform after the impact should preserve sufficient load carrying capacities to resist environmental and functional loads before it is repaired.

It can be very challenging both numerically and physically to pursue structural behavior until total collapse of the system; e.g., significant uncertainties exist regarding actual ductility limits for members and joints and how to model them in theoretical analyses. Hence, it has become customary to design components and subsystems to resist characteristic ship collision actions and relevant permanent and environmental loads both during damage and in post-damage conditions so that they undergo substantial damage, but still have considerable margins against complete failure.

The design of platform braces/legs against ship impacts may be carried out in the ductile, shared-energy or strength design domain (DNV-RP-C204, 2010) (see Fig. 29):

Strength design: The installation is strong enough to resist collision forces with minor deformation, so that the ship is forced to deform and dissipate the major part of the energy.

Ductility design: The installation undergoes large plastic deformation and dissipates the major part of the collision energy.

Shared energy design: Both the installation and the ship contribute significantly to energy dissipation.

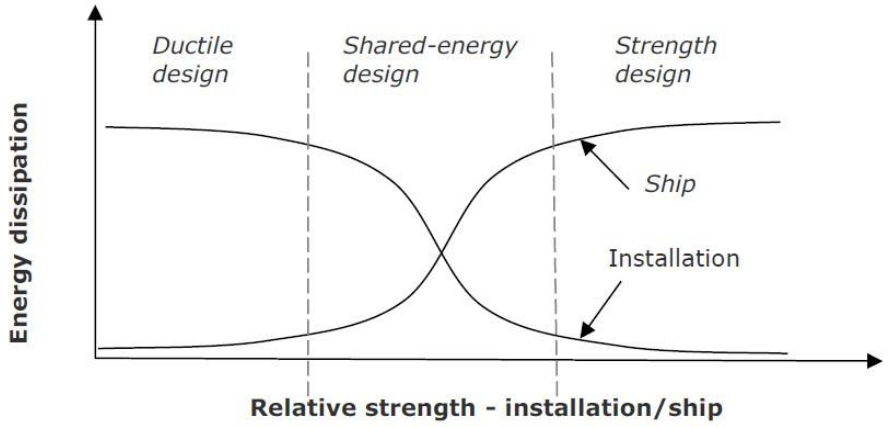

Fig. 29. Energy dissipation for strength, ductile and shared-energy design, from DNV-RP-C204 (2010)

The governing factor is the resistance to plastic collapse in bending, R_0. If the resistance is larger than the force that the ship will produce when penetrated by a rigid tube, the ship will predominantly dissipate the collision energy, i.e. the brace/leg response is in the strength domain. However, the brace/leg must also comply with local denting compactness requirements; otherwise, the ship's resistance to penetration will be larger than the residual bending collapse resistance of a dented tube. If R_0, is less than the ship's resistance to penetration, the brace/leg will be in the shared-energy or ductile domain. Depending on the brace/leg dimensions and material strength, it may dissipate considerable energy by beam bending and membrane forces at large deformations. Local denting will contribute to the energy dissipation as well. However, it may be advisable to avoid significant local denting because local denting reduces total energy absorption and responses for denting beyond brace/leg radius are uncertain. With little denting, simple equations apply.

As stated before, unless further evaluations are performed, the kinetic energy for a bow impact should be 50 MJ according to the new version NORSOK N003 standard (NORSOK, 2017). This energy level cannot be absorbed by a single brace or leg. A viable option is to design the braces to have sufficient strength to penetrate the bow so that the ship can dissipate considerable energy, which falls into the shared energy or strength design domain.

9.2 Ship platform interaction

Within the shared energy domain, the response and energy absorption of the striking and struck objects are very sensitive to their relative strengths, and failure of a single structural component may turn the strong structure into the weak. To capture the ship-platform interactions accurately, an integrated analysis of platform and ship structures modeled with shell elements is required. Proper modelling of the material properties and fracture is essential (refer to *Section 2.2*).

During collisions, the softer structure will deform and the impact force will be distributed over a larger contact area. This increases the resistance of the strong structure, and therefore there will be an upward shift of the resistance curve to the stronger structure as shown in Fig. 30. In designing offshore platforms, the load-deformation curves of ships and platforms are often established independently by disregarding the relative strength and assuming that the other object

is infinitely rigid. Shared energy design based on such independently obtained force curves may not yield the correct energy distributions.

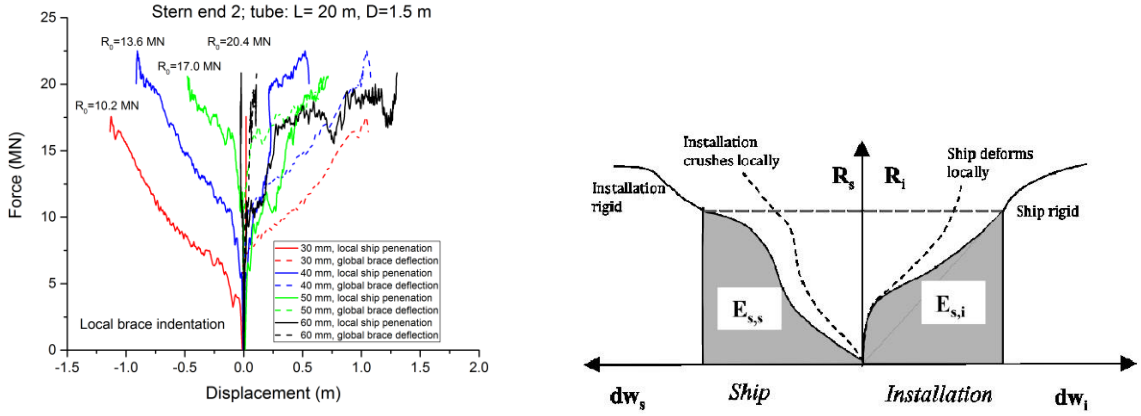

Fig. 30. (a) Force-local deformation curve for a ship stern impacted by vertical braces with 1.5 m diameters and varying thicknesses; from Yu and Amdahl (2018); (b) Dissipation of strain energy in the ship and platform; from DNV RP C204 (DNV-GL, 2018), see also ABS (2013)

To account for the ship-platform interactions, the new version DNV-GL RP C204 (DNV-GL, 2018) treats it empirically by introducing an energy dissipation correction factor β such that:

$$E_s = \beta \int_0^{w_{s,\max}} R_s dw_s + \int_0^{w_{i,\max}} R_i dw_i \tag{29}$$

where R_S and R_i are the deformation resistances of the ship and the installation, respectively. $0<\beta<1$ limits the energy dissipation capability of the structure.

Travanca and Hao (2015) tried three parameters k_s / m_0, k_s / k_i and R_c to represent the relative strengths of a striking ship and the struck installation and plotted energy dissipation proportions versus the relative strength factors based on numerical simulation. k_s and k_i are the tangential stiffness of the force-displacement curves of the ship and installation, respectively. They found that the thickness of the installation tubes played an important role in determining the platform energy absorption and that plastic bending moment of tube walls per unit width $m_0 = 1/4\sigma_y t^2$ could therefore be used to describe the platform relative strength.

It is difficult to find the proportion of energy dissipation in a platform and ship using simple methods. During a ship collision, the weaker structure may shift several times from one to the other in shared energy design. The new version DNV-GL RP C204 (DNV-GL, 2018) relates the amount of energy dissipation in a ship bow to the collapse resistance in bending for the brace, R_0, as shown in Table 1 provided that the compactness requirement is satisfied. The results shown in the table are based on a conservative consideration of a series of numerical simulation results. This share of energy dissipation has not been extended to ship stern- and broad side impacts.

Table 1. Energy dissipation in standard OSV bows versus brace resistance from DNV-GL RP C204 (DNV-GL, 2018)

Contact location	**Energy dissipation in bow if brace resistance R_0**				
	> 6 MN	**> 8 MN**	**> 10 MN**	**> 12 MN**	**> 18 MN**
On bulb vertical brace	-	-	-	3 MJ	Large
On bulb oblique brace				Large	Large
Above bulb	5 MJ	7 MJ	11 MJ	Large	Large
First deck	2 MJ	4 MJ	17 MJ	Large	Large
First deck - oblique brace	2 MJ	4 MJ	17 MJ	Large	Large
Between forecastle/ first deck	5 MJ	10 MJ	15 MJ	Large	Large
Arbitrary location	**2 MJ**	**4 MJ**	**11 MJ**	**3 MJ or Large**	**Large**

9.3 Compactness requirements against excessive local dents

A few requirements exist in the literature for a brace/leg to maintain compactness during deformation. Sherman (1976) suggested that members with D/t of 35 or less and L/D up to 22 can be deemed to maintain full bending capacity during deformation based on experimental observations.

The API rules (API-RP2A, 1977) prescribe $D/t < 9000/\sigma_y \left(\sigma_y \text{ in MPa}\right)$ to maintain full capacity trough plastic deformation. For $9000/\sigma_y < D/t < 15200/\sigma_y$, a limited plastic rotation capacity can be assumed.

The current NORSOK N004 (NORSOK, 2004) and DNV-GL RP C204 (DNV-RP-C204, 2010) require the following compactness criterion to avoid excessive local denting of the tube before forming a three-hinge collapse mechanism:

$$R_0 / R_c < 6 \tag{30}$$

This criterion was shown to be overly conservative in Storheim and Amdahl (2014) based on observations of numerical simulation results. They proposed to use R_c as a characteristic strength factor. The R_c criterion was proved to be useful in Travanca and Hao (2015) through a series of numerical simulation.

Cerik et al. (2016) carried out a series of impact experiments and numerical simulations to study the responses of tubular members subjected to mass impacts. A classification of the impact responses of tubular members is suggested by using the indicator of R_0/R_c. The following four response categories are suggested:

Mode 1: $R_0 / R_c < 6.5$; dominated by global bending

Mode 2: $6.5 \le R_0 / R_c \le 10$; dominated by both local denting and beam deformation, and local denting ceases immediately after plastic collapse.

Mode 3: $10 \le R_0 / R_c \le 23;$ dominated by both local denting and beam deformation, and local denting continues after plastic collapse.

Model 4: $R_0 / R_c > 23;$ dominated by local shell denting.

Yu and Amdahl (2018) found that the D/t and L/D requirements and the R_0/R_c criterion actually limited the transition indentation to a small value (refer to *Section 5.3*), but may not restrict the development of local denting in the beam bending stage. They suggested using the R_c criterion following the recommendations of Storheim and Amdahl (2014) and related to the maximum collision force F_{max} when a ship's bow crushes a rigid brace/leg:

$$R_c \ge 1.9 \frac{F_{\max}}{24} \tag{31}$$

The criterion in Eq. (31) was shown to be useful for limiting the development of local indentation in the bending stage as well as through a series of numerical simulations. R_c is suggested to be 1.2 MN for stern corner impacts, and 1.5 MN for stern end impacts. The compactness criteria require more validation.

9.4 Residual strength of damaged platforms

Platforms after ship collision damage should be able to withstand operational loads and certain environmental loads without progressive collapse of the structures. The strength capacities of damaged platforms should be checked (refer to Fig. 31). DNV RP C104 (DNV, 2012) and API RP2A-WSD (API-RP2A-WSD, 2014) require that a damaged platform shall survive environmental loads corresponding to a return period of no less than 1 year. A more strict criterion is to require the damaged platform to survive the environmental loads with an annual exceedance probability of 10^{-2} according to Moan (2009), which corresponds to the requirement for ultimate limit state design of an intact platform; however, in the damaged state, the partial safety factors for loads and resistance can be taken as equal to unity.

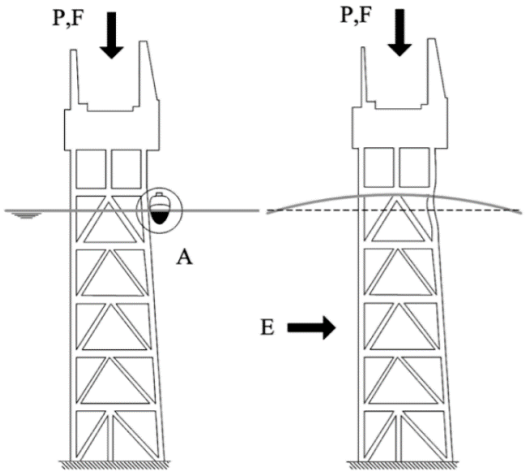

Fig. 31. Two-step Accidental Collapse Limit State check of global failure, considering accidental (A), Environmental (E), functional (F) permanent (P) actions; from Moan (2009)

A simple, albeit conservative approach, is to remove the struck member by assuming that it is completely ineffective after damage and then to undertake a push-over analysis to check the platform residual strength; refer to e.g. Amdahl and Johansen (2001). For dented tubes, a few formulations exist (refer to e.g. Taby (1986) and Ellinas (1984)) that allow taking post-damage strength into account. Naderi et al. (2009) carried out a static pushover analysis of a jacket platform under both intact and damaged conditions using USFOS. The platform was a four-legged production jacket with K-braced frames located in the Persian Gulf. The investigated damage on tubular structures encompassed dent depths of 0.25D, 0.50D and 0.75D or out-of-straightnesses of 0.5%, 0.75%, 1.2% and 1.4%. The results showed that the damaged platform had considerable redundancy to withstand external loads through force redistributions, and the failure of one component would generally not limit the capacity of the structure as a whole. The reserve capacity of an intact platform can be described by the reserve resistance factor (REF):

$$\text{REF} = \frac{\text{Environmental loads at collapse (undamaged)}}{\text{Design environmental loads}} \tag{32}$$

The residual strength of a damaged offshore platform may be represented by the residual strength factor (RSF), which is defined as:

$$\text{RSF} = \frac{\text{Environmental loads at collapse (damaged)}}{\text{Design environmental loads}} \tag{33}$$

According to Naderi et al. (2009), the RSFs with failure of one member for the investigated jacket ranged over 1.4 to 2.1 depending on damage type, extent and location, where the design loads were selected as wave loads with a return period of 100 years. The RSFs for an eight-legged North Sea jacket can range over 3.1-4.4 according to Ghose et al. (1994). Similar conclusions were reported by Sveen (1990) when a West German submarine collided with the eight-legged Oseberg B jacket on the Norwegian Continental Shelf in 1988, the estimated energy of which was 5-6 MJ. Collapse analysis of the damaged platform revealed high reserve strengths (an RSF of approximately 2.3) for the jacket structure. Failure of several tubular members will further reduce the residual capacity of a damaged platform and threaten its global integrity. An example is the Big Orange-Ekofisk 2-4/W collision (PSA, 2009), after which the jacket had to be dismantled. Billington et al. (1993) reviewed reserve, residual and ultimate strength analyses of offshore structures before the 1990s. The methods, including analytical, experimental and nonlinear finite element analyses, used to evalutate the reserve and residual strengths of offshore platforms were summarized. In addition to the damaged members, the influence of nonlinear joint behavior, platform foundations and realistic load distributions were highlighted.

In general, ship collisions take place around the mean water level. Hence, a platform's global resistance to environmental loads is only moderately affected because a significant part of the wave loads enters below the collision zone. It is also essential for the residual strength such that the platform can allow for a complete loss of load carrying by the damaged legs, either by redistributing the topside loads by diagonals to the adjacent legs, as is the case for the platform in Fig. 32, or by the topside framework. Note that only two legs must carry the total topside loads for the damaged jacket in Fig. 32.

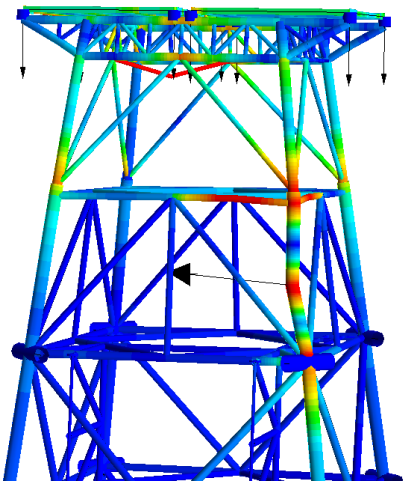

Fig. 32. A four-legged jacket subjected to a collision

10. Conclusions and recommendations

This paper presents a review of the structural response and design of offshore tubular structures subjected to ship impacts. From the point of view of platform crashworthiness design, significant changes have taken place since the first DNV rule for ship collisions in the 1980s, notably the increased impact energy due to larger vessels and impact speeds, and new ship designs such as bulbous bows, X-bows and ice strengthened vessels. This has triggered a revision to the DNV RP C204 in 2017. The standard design energy has increased significantly to 50 MJ for bow impacts, 28 MJ for broad side collisions and 22 MJ for stern collisions in the new version NORSOK N003 standard. To absorb such large amounts of energy, *strength design* or *shared-energy* design may be required, for which a struck brace or leg must be capable of penetrating the bow such that the ship dissipates considerable energy.

Collision analysis is often considered to be centric; i.e., the impact force is directed through the center of gravity of the ship and floating platforms. This is often a very credible scenario, but sometimes it is overly conservative because part of the impact energy may be transferred into other motion components (e.g., sway, roll, yaw and pitch). External dynamics methods have been developed that often provide approximate but useful results for general eccentric collisions. External dynamic models should be used with care for ship collisions with offshore braces and legs because tubular members may penetrate into the striking ship bow and lock the ship motions. The dissipated energy predicted by external dynamic models can be much underestimated. For cases with complex ship motions, long durations, or potential motion locking, the coupled simulation method based on beam/shell modeling with beam elements representing the global motion of the ship is promising and should be further developed. Any secondary impacts should also be considered in eccentric collisions.

Jackets installed in shallow and moderately deep water are generally dominated by static responses. Deep water jackets and notably jack-ups, are more compliant and may absorb a considerable part of the energy by elastic deformation. Ship collision assessments of such platforms should be carried out using dynamic analysis. During a collision, energy absorption in

the platform occurs mainly through lateral deformation of the struck and adjacent members, buckling of compressed members and global motions of the platform. The deformations of laterally impacted unstiffened tubular members will exhibit three deformation stages: local denting, global bending and membrane stretching. The underlying mechanics of tube deformation and the ultimate strength of damaged tubes and platforms have been reviewed. It was found that existing simplified models captured the main features of the denting process and the residual capacity of dented members subjected to bending and compression. Such models have been implemented in the beam-column element formulation in the USFOS computer program.

Cross-sectional denting will significantly degrade the bending capacities of tubular members. Therefore, in order to obtain *strength design*, it is essential to design a brace or leg so that it does not undergo large denting. The extent of the local dent before entering the global bending stage can be described by the denting transition ratio. Compactness requirements in the literature were reviewed, and the characteristic denting resistance factor R_c was adopted as a compactness indicator in the new version DNV GL RP C204.

If the strengths of the platform and ship fall in the shared energy domain, significant ship platform interactions will occur and local denting of the struck tube will increase the ship's resistance to penetration. The ship platform interaction effect is considered in the new version DNV GL RP C204 standard by introducing a correction factor β that is related to the denting resistance R_c of tubulars. The procedure developed to account for the interaction effect is simplified. If more accurate calculations are required, it is always possible to conduct NLFEA simulations with shell element modelling of the hit member and the ship using explicit programs such as LS-DYNA and ABAQUS. Modelling ship structures is somewhat demanding. The finite element library of a few supply vessels, established by DNV GL and made available to the engineering community is very valuable for this purpose, and it also standardizes the vessels used by different companies. This will enhance greatly the use of explicit NLFEA in the future.

The boundary conditions adopted for collision simulations need to be considered carefully. Alternatively, analyses may be carried out using complete platform models. Preferably, hybrid shell/beam models should be used such that beam elements are utilized outside the region of primary damage. Depending on the studied problem and platform configurations, shell modelling of several members and joints may be needed. Columns subjected to compression should contain imperfections that are carefully calibrated to code column curves. Shell modelling of tubular joints is cumbersome, but it will allow for collision simulations against tubular joints where little information exists regarding resistance to impact. It is also noted that tubular joints modelled with shell elements will generally produce ultimate bending capacities larger than those predicted by USFOS in which joint strength is based on code formulations because the codes neglect the strengthening effect of multi-planar joints.

Because collision forces in most cases are considerably smaller than the extreme environmental loads, soil capacity will most often not be challenged. In such cases, analysts can be significantly eased by skipping pile-soil modeling and using pinned boundary conditions at the mud line. This is generally conservative.

NLFEA may be needed if contact takes place close to brace ends because the simplified dent models that have been developed may not be representative for behaviors in such cases. There is room for the improvement of simplified methods for the determination of indentation resistance of ring- and/or axially stiffened columns, e.g., for semi-submersibles. The formulations proposed have so far considered a knife-edged rigid indenter. For stern corner and bow/bulb impacts, contact forces will be more concentrated and the formulations for knife-edge indenters may overpredict the resistance.

Precise prediction of fracture is essential with respect to damage prediction and opening of compartments to flooding or cargo spills. Several models have been proposed and compared with experiments, but room for improvement remains significant.

Acknowledgments

This work has been funded by the Research Council of Norway (RCN) through the Centers of Excellence funding scheme, project AMOS (Grant number 223254) at the Norwegian University of Science and Technology (NTNU). This support is gratefully acknowledged by the authors.

References

Abramowicz, W., 2003. Thin-walled structures as impact energy absorbers. Thin-Walled Structures 41 (2), 91-107.

Abramowicz, W., Jones, N., 1986. Dynamic progressive buckling of circular and square tubes. International Journal of Impact Engineering 4 (4), 243-270.

Abramowicz, W., Jones, N., 1997. Transition from initial global bending to progressive buckling of tubes loaded statically and dynamically. International Journal of Impact Engineering 19 (5), 415-437.

ABS-MODU, 2012. Rules for Building and Classing Mobile Offshore Drilling Units. 1997.

ABS, 2013. Guidance notes on accidental load analysis and design of offshore structures.

Alexander, J., 1960. An approximate analysis of the collapse of thin cylindrical shells under axial loading. The Quarterly Journal of Mechanics and Applied Mathematics 13 (1), 10-15.

Alghamdi, A.A.A., 2001. Collapsible impact energy absorbers: an overview. Thin-Walled Structures 39 (2), 189-213.

Allan, J.D., 1992. The effect of ship impact on the load carrying capacity of steel tubes / J.D. Allan and J. Marshall. HMSO, London.

Alsos, H.S., Hopperstad, O.S., Törnqvist, R., Amdahl, J., 2008. Analytical and numerical analysis of sheet metal instability using a stress based criterion. International Journal of Solids and Structures 45 (7), 2042-2055.

Amdahl, J., 1980. Impact Capacity of Steel Platforms and Tests on Large Deformations of Tubes and Transverse Loading. Det norske Veritas, Progress Report (10), 80-0036.

Amdahl, J., 1983. Energy absorption in ship-platform impacts, Doctoral Thesis, Norwegian Institute of technology.

Amdahl, J., Eberg, E., 1993. Ship collision with offshore structures, Proceedings of the 2nd European Conference on Structural Dynamics (EURODYN'93), Trondheim, Norway, June, pp. 21-23.

Amdahl, J., Holmas, T., 2016. ISUM for Offshore Frame Structures, ASME 2016 35th International Conference on Ocean, Offshore and Arctic Engineering. American Society of Mechanical Engineers, pp. V009T013A014-V009T013A014.

Amdahl, J., Johansen, A., 2001. High-energy ship collision with jacket legs, The Eleventh International Offshore and Polar Engineering Conference. International Society of Offshore and Polar Engineers.

Amdahl, J., Søreide, T.H., 1981. Energy absorption in axially compressed cylindrical shells with special reference to bulbous bows in collision. Division of Marine Structures, Norwegian Institute of Technology.

Amdahl, J., Watan, R., Hu, Z., Holmås, T., 2012. Broad side ship collision with jacket legs: Examination of NORSOK N-004 Analysis Procedure, ASME 2012 31st International Conference on Ocean, Offshore and Arctic Engineering. American Society of Mechanical Engineers, pp. 745-751.
Andrews, K., England, G., Ghani, E., 1983. Classification of the axial collapse of cylindrical tubes under quasi-static loading. International Journal of Mechanical Sciences 25 (9-10), 687-696.
API-RP2A-WSD, 2014. Recommended practice for planning, designing and constructing fixed offshore platforms–working stress design–, Twenty-.
API-RP2A, 1977. API recommended practice for planning, designing, and constructing fixed offshore platforms. American Petroleum Institute, Production Dept.
Azadi, M.R.E., 1998. Analysis of static and dynamic pile-soil-jacket behaviour. Department of Marine Structures, Faculty of Marine Technology, Norwegian University of Science and Technology, Trondheim.
Azadi, M.R.E., 2007. The influence of different scenarios of supply ship collision on the dynamic response of a north-sea jacket-pile-soil system, ASME 2007 26th International Conference on Offshore Mechanics and Arctic Engineering. American Society of Mechanical Engineers, pp. 19-26.
Billingham, J., Sharp, J., Spurrier, J., Kilgallon, P., 2003. Review of the performance of high strength steels used offshore. Health Saf. Exec 111.
Billington, C.J., Bolt, H.M., Ward, J.K., 1993. Reserve, Residual And Ultimate Strength Analysis of Offshore Structures:State of the Art Review. International Society of Offshore and Polar Engineers.
BS-EN-10225, 2009. 10225: Weldable structural steels for fixed offshore structures—Technical delivery conditions. London: British Standard Institution.
Buldgen, L., Le Sourne, H., Pire, T., 2014. Extension of the super-elements method to the analysis of a jacket impacted by a ship. Marine Structures 38, 44-71.
Cai, J., Jiang, X., Lodewijks, G., 2017. Residual ultimate strength of offshore metallic pipelines with structural damage–a literature review. Ships and Offshore Structures, 1-19.
Calle, M.A., Verleysen, P., Alves, M., 2017. Benchmark study of failure criteria for ship collision modeling using purpose-designed tensile specimen geometries. Marine Structures 53, 68-85.
Cerik, B.C., Shin, H.K., Cho, S.-R., 2015. On the resistance of steel ring-stiffened cylinders subjected to low-velocity mass impact. International Journal of Impact Engineering 84, 108-123.
Cerik, B.C., Shin, H.K., Cho, S.-R., 2016. A comparative study on damage assessment of tubular members subjected to mass impact. Marine Structures 46, 1-29.
Cho, S.-R., Kwon, J.-S., Kwak, D.-I., 2010. Structural Characteristics of Damaged Offshore Tubular Members. Journal of Ocean Engineering and Technology 24 (4), 1-7.
Cho, S.R., 1987. Design approximations for offshore tubulars against collisions. PhD Thesis, Glasgow University, UK.
Cho, S.R., 1990. Development of a simplified dynamic analysis procedure for offshore collisions. Bulletin of the Society of Naval Architects of Korea 27 (4), 72-82.
Choung, J., Nam, W., Lee, J.-Y., 2013. Dynamic hardening behaviors of various marine structural steels considering dependencies on strain rate and temperature. Marine Structures 32, 49-67.
Consolazio, G., Lehr, G., McVay, M., 2003. Dynamic finite element analysis of vessel-pier-soil interaction during barge impact events. Transportation Research Record: Journal of the Transportation Research Board (1849), 81-90.
Cowper, G.R., Symonds, P.S., 1957. Strain-hardening and strain-rate effects in the impact loading of cantilever beams. Brown Univ Providence Ri.
de Oliveira, J., Wierzbicki, T., Abramowicz, W., Veritas, N., 1982. Plastic Behaviour of Tubular Members Under Lateral Concentrated Loading. Det norske Veritas, Research Division.
De Oliveria, J., 1981. The behavior of steel offshore structures under accidental collisions, Offshore Technology Conference. Offshore Technology Conference.
DNV-GL, 2018. Recommended practice DNV-RP-C204. DET NORSKE VERITAS.
DNV-OS-B101, 2009. DNV-OS-B101 Metallic Materials.
DNV-RP-C204, 2010. Recommended practice DNV-RP-C204. DET NORSKE VERITAS.

DNV-RP-C208, 2016. Determination of Structural Capacity by Non-linear FE analysis Methods. DET NORSKE VERITAS.
DNV, 2012. Recommended Practice DNV-RP-C104 Self-elevating Units. RP-C104.
Duan, L., Chen, W., Loh, J., 1993. Analysis of dented tubular members using moment curvature approach. Thin-Walled Structures 15 (1), 15-41.
Duan, L., Loh, J., Chen, W., 1990. Moment-Thrust-Curvature Relationships for Dented Tubular Section. Report No. CE-STR-90-26, School of Civil Engineering, Purdue University, West Lafayette, IN.
Durkin, S., 1987. An analytical method for predicting the ultimate capacity of a dented tubular member. International Journal of Mechanical Sciences 29 (7), 449-467.
Ehlers, S., Broekhuijsen, J., Alsos, H.S., Biehl, F., Tabri, K., 2008. Simulating the collision response of ship side structures: A failure criteria benchmark study. International Shipbuilding Progress 55 (1-2), 127-144.
Ellinas, C., Valsgard, S., 1985. Collisions and damage of offshore structures: a state-of-the-art. Journal of energy resources technology 107 (3), 297-314.
Ellinas, C.P., 1984. Ultimate strength of damaged tubular bracing members. Journal of Structural Engineering 110 (2), 245-259.
Ellinas, C.P., 1995. Mechanics of ship/jack-up collisions. Journal of Constructional Steel Research 33 (3), 283-305.
Ellinas, C.P., Walker, A.C., 1983. Damage on offshore tubular bracing members, IABSE Colloquium on Ship Collisions With Bridges and Offshore Structures, Copenhagen, May, pp. 253-261.
Fatt, H., Wierzbicki, T., 1991. Denting analysis of ring stiffened cylindrical shells. International Journal of Offshore and Polar Engineering 1 (02).
Foss, G., Edvardsen, G., 1982. Energy Absorbtion During Ship Impact on Offshore Steel Structures, Offshore Technology Conference. Offshore Technology Conference.
Furnes, O., Amdahl, J., 1980. Ship collisions with offshore platforms. Intermaritec'80.
Gerard, G., 1958. The crippling strength of compression elements. J. of the Aeronautical Science.
Ghose, D.J., Nappi, N.S., Wiernicki, C.J., 1994. Residual Strength of Damaged Marine Structures. DESIGNERS AND PLANNERS INC ARLINGTON VA.
Gjerde, P., Parsons, S., Igbenabor, S., 1999. Assessment of jack-up boat impact analysis methodology. Marine Structures 12 (4), 371-401.
Guedes Soares, C., Søreide, T.H., 1983. Plastic analysis of laterally loaded circular tubes. Journal of Structural Engineering 109 (2), 451-467.
Guillow, S.R., Lu, G., Grzebieta, R.H., 2001. Quasi-static axial compression of thin-walled circular aluminium tubes. International Journal of Mechanical Sciences 43 (9), 2103-2123.
Hallquist, J.O., 2006. LS-DYNA theory manual. Livermore software Technology corporation 3, 25-31.
Harding, J.E., Onoufriou, A., 1995. Behaviour of ring-stiffened cylindrical members damaged by local denting. Journal of Constructional Steel Research 33 (3), 237-257.
Haris, S., Amdahl, J., 2012. An analytical model to assess a ship side during a collision. Ships and Offshore Structures 7 (4), 431-448.
Haris, S., Amdahl, J., 2013. Analysis of ship–ship collision damage accounting for bow and side deformation interaction. Marine Structures 32 (Supplement C), 18-48.
Hibbitt, Karlsson, Sorensen, 2001. ABAQUS/standard User's Manual. Hibbitt, Karlsson & Sorensen.
Hogström, P., Ringsberg, J.W., 2012. An extensive study of a ship's survivability after collision–A parameter study of material characteristics, non-linear FEA and damage stability analyses. Marine Structures 27 (1), 1-28.
Hong, L., Amdahl, J., Wang, G., 2009. A direct design procedure for FPSO side structures against large impact loads. Journal of Offshore Mechanics and Arctic Engineering 131 (3), 031105.
HSE, 2004. RR220-Ship collision and capacity of brace members of fixed steel offshore platforms. Health and Safety Executive.
ISO, 2007. 19902: 2008-07: Petroleum and natural gas industries–Fixed steel offshore structures (ISO 19902: 2007). English version EN ISO 19902, 182-202.

Jin, W.-l., Song, J., Gong, S.-f., Lu, Y., 2005. Evaluation of damage to offshore platform structures due to collision of large barge. Engineering Structures 27 (9), 1317-1326.
Johnson, W., Soden, P., Al-Hassani, S., 1977. Inextensional collapse of thin-walled tubes under axial compression. The journal of strain analysis for engineering design 12 (4), 317-330.
Jones, N., 1989. Some comments on the modelling of material properties for dynamic structural plasticity. Mechanical Properties of Materials at High Rates of Strain 1989, 435-445.
Jones, N., 2011. Structural impact. Cambridge university press.
Jones, N., Birch, R., 1996. Influence of internal pressure on the impact behavior of steel pipelines. Journal of pressure vessel technology 118 (4), 464-471.
Jones, N., Birch, R., 2010. Low-velocity impact of pressurised pipelines. International Journal of Impact Engineering 37 (2), 207-219.
Jones, N., Birch, S., Birch, R., Zhu, L., Brown, M., 1992. An experimental study on the lateral impact of fully clamped mild steel pipes. Proceedings of the Institution of Mechanical Engineers, Part E: Journal of Process Mechanical Engineering 206 (2), 111-127.
Jones, N., Shen, W., 1992. A theoretical study of the lateral impact of fully clamped pipelines. Proceedings of the Institution of Mechanical Engineers, Part E: Journal of Process Mechanical Engineering 206 (2), 129-146.
Jones, N., Uran, T.O., Tekin, S.A., 1970. The dynamic plastic behavior of fully clamped rectangular plates. International Journal of Solids and Structures 6 (12), 1499-1512.
Karagiozova, D., Alves, M.l., 2004. Transition from progressive buckling to global bending of circular shells under axial impact—Part I: Experimental and numerical observations. International Journal of Solids and Structures 41 (5), 1565-1580.
Karagiozova, D., Jones, N., 2008. On the mechanics of the global bending collapse of circular tubes under dynamic axial load—Dynamic buckling transition. International Journal of Impact Engineering 35 (5), 397-424.
Karroum, C.G., Reid, S.R., Li, S., 2007a. Indentation of ring-stiffened cylinders by wedge-shaped indenters—Part 1: An experimental and finite element investigation. International Journal of Mechanical Sciences 49 (1), 13-38.
Karroum, C.G., Reid, S.R., Li, S., 2007b. Indentation of ring-stiffened cylinders by wedge-shaped indenters—Part 2: Scale model tests. International Journal of Mechanical Sciences 49 (1), 39-53.
Khedmati, M.R., Nazari, M., 2012. A numerical investigation into strength and deformation characteristics of preloaded tubular members under lateral impact loads. Marine Structures 25 (1), 33-57.
Kim, K.J., Lee, J.H., Park, D.K., Jung, B.G., Han, X., Paik, J.K., 2016. An experimental and numerical study on nonlinear impact responses of steel-plated structures in an Arctic environment. International Journal of Impact Engineering 93 (Supplement C), 99-115.
Kvitrud, A., 2011. Collisions between platforms and ships in Norway in the period 2001-2010, ASME 2011 30th International Conference on Ocean, Offshore and Arctic Engineering. American Society of Mechanical Engineers, pp. 637-641.
Le Sourne, H., Barrera, A., Maliakel, J.B., 2015. Numerical crashworthiness analysis of an offshore wind turbine jacket impacted by a ship. Journal of Marine Science and Technology 23 (5), 694-704.
Le Sourne, H., Pire, T., Hsieh, J.R., Rigo, P., 2016. New analytical developments to study local and global deformations of an offshore wind turbine jacket impacted by a ship Proceedings of the 7th International Conference on Collision and Grounding of Ships and Offshore Structures (ICCGS2016), Ulsan, South Korea.
Levanger, H., Notaro, G., Hareide, J., O, 2016. Collision response and residual strength of jack up structure. Proceedings of PRADS 2016, Copenhagen, Denmark.
Li, M., Chandra, A., 1999. Influence of strain-rate sensitivity on necking and instability in sheet metal forming. Journal of materials processing technology 96 (1), 133-138.
Liu, Z., Amdahl, J., 2010. A new formulation of the impact mechanics of ship collisions and its application to a ship–iceberg collision. Marine Structures 23 (3), 360-384.

Ma, X., Stronge, W., 1985. Spherical missile impact and perforation of filled steel tubes. International Journal of Impact Engineering 3 (1), 1-16.
Makris, N., Gazetas, G., 1992. Dynamic pile-soil-pile interaction. Part II: Lateral and seismic response. Earthquake engineering & structural dynamics 21 (2), 145-162.
Marinatos, J., Samuelides, M., 2015. Towards a unified methodology for the simulation of rupture in collision and grounding of ships. Marine Structures 42, 1-32.
Minorsky, V., 1958. An analysis of ship collisions with reference to protection of nuclear power plants. Sharp (George G.) Inc., New York.
Moan, T., 2009. Development of accidental collapse limit state criteria for offshore structures. Structural Safety 31 (2), 124-135.
Moan, T., Amdahl, J., 1989. Catastrophic failure modes of marine structures. Structural failure, 463-510.
Moan, T., Amdahl, J., Gerhard, E., 2017. Assessment of ship impact risk to offshore structures-new NORSOK N-003 guidelines. Marine Structures.
MSL Engineering Ltd, 1996. JIP Assessment criteria reliability and reserve strength of tubular joints. . DOC No.C14200R018 Rev0.
MSL Engineering Ltd, 2000. JIP Assessment criteria reliability and reserve strength of tubular joints. Phase II, Tubular joints-Nonlinear modelling algorithms for frame analysis. MSL document refC20400r014 rev1.
Naderi, B., Aghakouchak, A., Mirzaei, M., 2009. Residual Strength of Damaged Jacket Type Offshore Platform and the Effects of Local Repair. capa 2, 1.
Nishida, M., Tanaka, K., 2006. Experimental study of perforation and cracking of water-filled aluminum tubes impacted by steel spheres. International Journal of Impact Engineering 32 (12), 2000-2016.
Nogami, T., Konagai, K., 1986. Time domain axial response of dynamically loaded single piles. Journal of Engineering Mechanics 112 (11), 1241-1252.
Nordal, S., Grande, L., Janbu, N., 1985. Prediction of pile behavior. Division of Geotechnical engineering, NTH, Norway.
NORSOK-M-120, 2008. NORSOK M-120: Material data sheets for structural steels.
NORSOK, 2004. NORSOK Standard N004. Design of steel structures, Appendix A, design against accidental actions. Det Norske Veritas 2004.
NORSOK, 2017. Actions and action effects, N-003. Oslo: Norwegian Technology Standards Institution.
Notaro, G., Johansen, A., Selås, S., Nybø, T., 2015. Estimation of high energy collision response for jacket structures, Proceedings of the 34th International Conference on Ocean, Offshore and Arctic Engineering, St. Johns, Newfoundland, Canada.
Ohtsubo, H., Suzuki, K., 1994. The Crushing Mechanics of Bow Structure in Head on Collision (1st Report). Journal of the Society of Naval Architects of Japan 1994 (176), 301-308.
Olabi, A.G., Morris, E., Hashmi, M.S.J., 2007. Metallic tube type energy absorbers: A synopsis. Thin-Walled Structures 45 (7), 706-726.
Pacheco, L., Durkin, S., 1988. Denting and collapse of tubular members—a numerical and experimental study. International Journal of Mechanical Sciences 30 (5), 317-331.
Paik, J.-K., Shin, B.-C., 1989. Damage effects on the ultimate strength of offshore tubular members. Journal of Ocean Engineering and Technology 3 (2), 77-86.
Paik, J.K., Pedersen, P.T., 1995. Ultimate and crushing strength of plated structures. Journal of Ship Research 39 (3), 250-261.
Paik, J.K., Thayamballi, A.K., 2003. Ultimate limit state design of steel-plated structures. John Wiley & Sons.
Palmer, A., Neilson, A., Sivadasan, S., 2006. Pipe perforation by medium-velocity impact. International Journal of Impact Engineering 32 (7), 1145-1157.
Pedersen, P.T., 2010. Review and application of ship collision and grounding analysis procedures. Marine Structures 23 (3), 241-262.

Pedersen, P.T., 2013. Ship collisions against wind turbines, quays and bridge piers, Collision and Grounding of Ships and Offshore Structures—Proceedings of the 6th International Conference on Collision and Grounding of Ships and Offshore Structures, ICCGS, pp. 273-281.
Pedersen, P.T., Li, Y., 2009. On the global ship hull bending energy in ship collisions. Marine Structures 22 (1), 2-11.
Pedersen, P.T., Zhang, S., 1998. On impact mechanics in ship collisions. Marine Structures 11 (10), 429-449.
Petersen, M.J., Pedersen, P.T., 1981. Collisions between ships and offshore platforms, Offshore Technology Conference. Offshore Technology Conference.
PSA, 2009. Investigation report following collision between Big Orange XVIII and Ekofisk 2/4-W. The Petroleum Safety Authority Norway, investigation report.
Qvale, K.H., 2012. Analysis and Design of Columns in Offshore Structures subjected to Supply Vessel Beam Collisions. Master thesis Norwegian University of Science and Technology.
Ringsberg, J.W., Amdahl, J., Chen, B., Cho, S.R., Ehlers, S., Hu, Z., Kubiczek, M., Jan, Korgesaar, M., Liu, B., Marinatos, J.N., Niklas, K., Parunov, J., Quinton, B.W.T., Rudan, S., Samuelides, E., Soares, C.G., Tabri, K., Villavicencio, R., Yamada, Y., Yu, Z., Zhang, S., 2018. MARSTRUCT benchmark study on nonlinear FE simulation of an experiment of an indenter impact with a ship side-shell structure. Marine Structures.
Ronalds, B.F., Dowling, P.J., 1987. A denting mechanism for orthogonally stiffened cylinders. International Journal of Mechanical Sciences 29 (10), 743-759.
Sherman, D.R., 1976. Test of circular steel tubes in bending. Journal of the Structural Division 102 (11), 2181-2195.
Skallerud, B., Amdahl, J., 2002. Nonlinear analysis of offshore structures. Research Studies Press Baldock, Hertfordshire,, England.
Smith, C., 1982. Strength and stiffness of damaged tubular beam columns. Buckling of shells in offshore structures, 1-24.
Smith, C., Kirkwood, W., Swan, J., 1979. Buckling strength and post-collapse behaviour of tubular bracing members including damage effects, Proceedings of the Second International Conference on the Behaviour of Off-Shore Structures, held at Imperial College, London, England.
Smith, C., Somerville, W., Swan, J., 1980. Compression tests on full-scale and small-scale tubular bracing members including damage effects. OT-R8079, Department of Energy, UK.
Smith, C., Somerville, W., Swan, J., 1981. Residual strength and stiffness of damaged steel bracing members, Offshore Technology Conference. Offshore Technology Conference.
Soreide, T., Amdahl, J., Eberg, E., Hellan, O., Halmås, T., 1999. USFOS–a computer program for progressive collapse analysis of steel offshore structures. Theory Manual. SINTEF Report STF71 F 88038.
Søreide, T.H., Kavlie, D., 1985. Collision damages and residual strength of tubular members in steel offshore structure Shell strucctures stability and strength, 185-220.
Storheim, M., 2016. Structural Response in Ship-Platform and Ship-Ice Collisions.
Storheim, M., Alsos, H.S., Amdahl, J., 2017. Evaluation of Nonlinear Material Behavior for Offshore Structures Subjected to Accidental Actions, ASME 2017 36th International Conference on Ocean, Offshore and Arctic Engineering. American Society of Mechanical Engineers, pp. V03AT02A006-V003AT002A006.
Storheim, M., Amdahl, J., 2014. Design of offshore structures against accidental ship collisions. Marine Structures 37, 135-172.
Storheim, M., Amdahl, J., 2017. On the sensitivity to work hardening and strain-rate effects in nonlinear FEM analysis of ship collisions. Ships and Offshore Structures 12 (1), 100-115.
Storheim, M., Amdahl, J., Martens, I., 2015. On the accuracy of fracture estimation in collision analysis of ship and offshore structures. Marine Structures 44, 254-287.
Stronge, W.J., 2004. Impact mechanics. Cambridge university press.
Sun, B., Hu, Z., Wang, G., 2015. An analytical method for predicting the ship side structure response in raked bow collisions. Marine Structures 41, 288-311.

Sveen, D., 1990. Oseberg B Jacket-Damage Assessment and Repair After Submarine Collision. Journal of Petroleum Technology 42 (11), 1,421-421,425.
Tabri, K., 2012. Influence of coupling in the prediction of ship collision damage. Ships and Offshore Structures 7 (1), 47-54.
Taby, J., 1986. Ultimate and Post-Ultimate Strength of Dented Tubular Members. Norges Tekniske Hogskole, Univ. Trondheim, Rep. No. UR-86-50, Oct. 1986.
Taby, J., Moan, T., 1985. Collapse and residual strength of damaged tubular members. 4th International Conference on Behaviour of Offshore Structures (BOSS 1985).
Taby, J., Moan, T., Rashed, S., 1981. Theoretical and experimental study of the behaviour of damaged tubular members in offshore structures. Norwegian Maritime Research 9 (2), 26-33.
Tørnqvist, R., 2003. Design of crashworthy ship structures. Technical University of Denmark Kgns Lyngby,, Denmark.
Travanca, J., Hao, H., 2014a. Dynamics of steel offshore platforms under ship impact. Applied Ocean Research 47, 352-372.
Travanca, J., Hao, H., 2014b. Numerical analysis of steel tubular member response to ship bow impacts. International Journal of Impact Engineering 64, 101-121.
Travanca, J., Hao, H., 2015. Energy dissipation in high-energy ship-offshore jacket platform collisions. Marine Structures 40, 1-37.
Ueda, Y., Rashed, S., 1985. Behavior of damaged tubular structural members. Journal of energy resources technology 107 (3), 342-349.
Ueda, Y., Rashed, S., Nakacho, K., 1985. New efficient and accurate method of nonlinear analysis of offshore tubular frames (the idealized structural unit method). Journal of energy resources technology 107 (2), 204-211.
Ueda, Y., Rashed, S.M.H., 1984. The idealized structural unit method and its application to deep girder structures. Computers & Structures 18 (2), 277-293.
VanDerHorn, E., Wang, G., 2011. A statistical study on the material properties of shipbuilding steels. Sustainable Maritime Transportation and Exploitation of Sea Resources, 371-378.
Walker, A.C., McCall, S., Thorpe, T.W., 1987. Strength of damage ring and orthogonally stiffened shells—part I: Plain ring stiffened shells. Thin-Walled Structures 5 (6), 425-453.
Walker, A.C., McCall, S., Thorpe, T.W., 1988. Strength of damaged ring and orthogonally stiffened shells—Part II: T-ring and orthogonally stiffened shells. Thin-Walled Structures 6 (1), 19-50.
Wang, G., Spencer, J., Chen, Y., 2002. Assessment of a ship's performance in accidents. Marine Structures 15 (4–5), 313-333.
Wang, Z., Liu, K., Ji, C., Chen, D., Wang, G., Soares, C.G., 2016. Experimental and numerical investigations on the T joint of jack-up platform laterally punched by a knife edge indenter. Ocean Engineering 127, 212-225.
Watan, R., 2011. Analysis and Design of Columns in Offshore Structures subjected to Supply Vessel Collisions. Master thesis Norwegian University of Science and Technology.
Wierzbicki, T., Suh, M., 1988. Indentation of tubes under combined loading. International Journal of Mechanical Sciences 30 (3), 229-248.
Yamada, Y., Pedersen, P., 2008. A benchmark study of procedures for analysis of axial crushing of bulbous bows. Marine Structures 21 (2), 257-293.
Yang, P.D.C., Caldwell, J.B., 1988. Collision energy absorption of ships' bow structures. International Journal of Impact Engineering 7 (2), 181-196.
Yao, T., Taby, J., Moan, T., 1988. Ultimate strength and post-ultimate strength behavior of damaged tubular members in offshore structures. Journal of Offshore Mechanics and Arctic Engineering 110 (3), 254-262.
Yu, Z., 2017. Hydrodynamic and structural aspects of ship collisions. Doctoral thesis, Department of Marine Technology, Norwegian University of Science and Technology, Trondheim.
Yu, Z., Amdahl, J., 2016. Full six degrees of freedom coupled dynamic simulation of ship collision and grounding accidents. Marine Structures 47, 1-22.

Yu, Z., Amdahl, J., 2017. Discussion of assumptions behind the external dynamics models in ship collisions and groundings. submitted to jounal.
Yu, Z., Amdahl, J., 2018. Analysis and design of offshore tubular members against ship impacts. Marine Structures 58, 109-135.
Yu, Z., Amdahl, J., Storheim, M., 2016a. A new approach for coupling external dynamics and internal mechanics in ship collisions. Marine Structures 45, 110-132.
Yu, Z., Shen, Y., Amdahl, J., Greco, M., 2016b. Implementation of Linear Potential-Flow Theory in the 6DOF Coupled Simulation of Ship Collision and Grounding Accidents. Journal of Ship Research 60 (3), 119-144.
Zeinoddini, M., Harding, J., Parke, G., 1998. Effect of impact damage on the capacity of tubular steel members of offshore structures. Marine Structures 11 (4), 141-157.
Zeinoddini, M., Harding, J., Parke, G., 1999. Dynamic behaviour of axially pre-loaded tubular steel members of offshore structures subjected to impact damage. Ocean Engineering 26 (10), 963-978.
Zeinoddini, M., Harding, J.E., Parke, G.A.R., 2008. Axially pre-loaded steel tubes subjected to lateral impacts (a numerical simulation). International Journal of Impact Engineering 35 (11), 1267-1279.
Zeinoddini, M., Parke, G., Harding, J., 2002. Axially pre-loaded steel tubes subjected to lateral impacts: an experimental study. International Journal of Impact Engineering 27 (6), 669-690.
Zhang, R., Zhi, X.-d., Fan, F., 2018. Plastic behavior of circular steel tubes subjected to low-velocity transverse impact. International Journal of Impact Engineering 114, 1-19.
Zhang, S., Pedersen, P.T., Ocakli, H., 2015. Collisions damage assessment of ships and jack-up rigs. Ships and Offshore Structures 10 (5), 470-478.
Zhu, L., 1990. Dynamic inelastic behaviour of ship plates in collision. University of Glasgow.
Zhu, L., Liu, Q., Jones, N., Chen, M., 2017. Experimental Study on the Deformation of Fully Clamped Pipes under Lateral Impact. International Journal of Impact Engineering.